

Dear Prof. Marsh,

Please find attached the revised manuscript “Verification of the multi-layer SNOWPACK model with different water transport schemes” for possible publication in The Cryosphere.

For completeness, we include here first the point-by-point response to the reviews, although no changes have been made compared to the responses provided by us in the online discussion.

After the responses, we include a marked-up document highlighting all changes made to the manuscript. Due to a technical issue, the updated table and the caption of Figure 5 are not highlighted as changes.

Please note that we also had to correct some equations, as we found that they were not consistent regarding the units and definition of the grain size (m vs mm and radius vs diameter). These errors were not present in the source code of the model and do not affect the simulations.

Kind regards, on behalf of all co-authors,

Nander Wever

École Polytechnique Fédérale de Lausanne (EPFL)

Laboratory of Cryospheric Sciences

EPFL-ENAC-IIE-CRYOS

Station 2, GR-A0-444

CH-1015 Lausanne, Switzerland

Phone: +41 81 417 0270

Email: nander.wever@slf.ch

Web: <http://people.epfl.ch/nander.wever>

Reviewer 1

We would like to thank the reviewer for his detailed and helpful comments and remarks, of which some made us rethink parts of the analysis. We point out our detailed response to the issues raised by the reviewer below.

Major comments

In addition to comparisons discussed in this manuscript, suggestions of studies to reduce discrepancies should be discussed for future reference. It will be informative to decide what observation and experiment is necessary to improve SNOWPACK model.

This is an interesting suggestion and we will amend the manuscript with an outlook section. We think that the recommendations for future research to improve the model, that seem most relevant in the context of this manuscript, can be separated into two parts: (i) the liquid water flow and (ii) melt behaviour in spring.

(i) Currently, simulating liquid water flow only considers a 1-dimensional component, assuming homogeneity in the horizontal dimensions. This is, however, a very strong simplification, as in reality, liquid water flow exhibits strong variation in 3 dimensions, due to preferential flow paths or flow fingering. Numerical experiments (Hirashima et al., 2014) and laboratory observations (Katsushima et al., 2013) have provided indications that these processes can be described using Richards equation in 3 dimensions. At the same time, several processes that do appear in 1-dimensional simulations, as for example the ponding of liquid water on capillary barriers, seem to be essential in forming preferential flow paths. This possibly allows for a parametrisation of preferential flow in the SNOWPACK model, that is closely linked to physical processes. Validation could be achieved by more detailed snow lysimeter studies, for example from measurement sites with multiple neighbouring lysimeters, improved laboratory experiments or further exploiting the upGPR data.

(ii) At the measurement site WFJ, we found a consistent overestimation of melt rates in spring, which is indicated by an underestimation of SWE compared to the manual snow profiles. The difficulty is that the SWE depletion in spring is dependent on many factors, such as snow density and wet snow settling, influencing snow heat capacity, internal heat fluxes and the penetration of short wave radiation, as well as the surface energy balance and liquid water flow. These processes are difficult to investigate separately. For the surface energy balance, ideally, repeated cold content measurements could be performed. This could be done using the calorimetric method: melting the snowpack and determining how much energy is required. However, these measurements are rather cumbersome to perform in the field. We are currently analysing measurements of turbulent fluxes, which so far have revealed that the constant flux layer assumption is often violated and it is hoped that an improved turbulent fluxes calculation scheme can be developed (Schlögl et al., 2015). Snow compaction (settling) in spring could be assessed with in-situ snow harps or snow profiles at a higher temporal resolution than only biweekly. However, recent advances in snow micro penetrometer (SMP) could also be helpful, allowing to achieve density measurements at high temporal and high spatial resolution with relatively little effort (Proksch et al., 2015). A drawback of that method is that SMP measurements are unfortunately not suitable for wet snow conditions. Finally, a more detailed analysis of upGPR data and snow lysimeter measurements can help to highlight discrepancies in the modelling of liquid water flow. Heilig et al. (2015) show an example of how bulk liquid water content measurements from upGPR in combination with snow lysimeter measurements could improve snowpack models.

However, in terms of wet snow area, residual water content seems to affect more rather than calculation scheme. According to author's previous paper (Wever et al., 2014), residual water content was not constant and not larger than 0.02. I think values or temporal variation of residual water content of bucket scheme and RE scheme should be shown in this paper. If the difference of θ_r between two schemes is large, discussions about suitable value of θ_r is also necessary.

The reviewer is using the term residual water content for both the bucket scheme and Richards equation. It is true that both water transport schemes have a parameter that may seem related to each other, but they are different. We therefore consistently used the terms water holding capacity or irreducible water content for the bucket scheme and residual water content for the Richards equation. The residual water content is a hypothetical value, principally not reached by water transport alone as it is associated with an infinitely small pressure head, but only due to phase changes. On the other hand, the water holding capacity in the bucket scheme refers to the typical liquid water content reached in snow, and refers to the size of the buckets. In RE, the actual liquid water content in the simulation is near or above the residual water content, whereas in the bucket scheme, the actual liquid water content is always at or below the water holding capacity. So the two values are not comparable. We will provide the following short note on this when revising the manuscript:

Note that the residual water content in the water retention curve, which is the dry limit, is not comparable to the water holding capacity or irreducible water content in the bucket scheme, which refers to wet conditions.

Specific comments

P8 In section 2.2, improvement of a calculation scheme for soil was discussed. It is one of the updated contents of the model in this paper. However, the effect of this improvement seems to be not shown in this paper. Is there large differences at the snow-soil boundary between before and after improvement of soil scheme? Probably it will be verified by comparison between simulated and observed soil water content profiles. It may be future works.

We did not compare the new soil module to the old one in the manuscript, as we think that this comparison is not important for the outcome of the manuscript. Basically, we did not intend to claim that the new soil module is better regarding the simulation of the snow-soil interface temperature, but only wanted to show that the approach is also providing a correct lower boundary condition for the snow cover. Both the old and the new model produce very similar results. Furthermore, the original soil module has been applied often in permafrost and rocky terrain, whereas we are interested in soils, as the upper part of the ground at Weissfluhjoch is soil rather than rock. We are indeed planning a comparison of soil moisture measurements, but as those measurements have not been carried out at Weissfluhjoch for logistical reasons, we consider it to be out of the scope of the manuscript.

P16 L20 Table1 showed average values for more than 10 years. I think it varies from year to year. Therefore, information of fluctuation from year to year is also necessary in Table 1. For example, standard deviation of annual average is calculated and added in Table 1 as 'average (\pm SD)'

This is an interesting suggestion, so we modified the table accordingly (see Table 1 in this document).

P19 L13 True, snowpack runoff is strongly coupled to the LWC distribution, but good agreement of runoff does not mean good agreement of water content in the snowpack. Do you have any water content profile data obtained in snow pit observation? Direct comparison of water content is important even if it is discontinuous and destructive.

We agree with the importance of verifying vertical liquid water content distributions inside the snowpack. For Weissfluhjoch, the only dataset available for the full studied period is the wetness reported by the observers from the biweekly manual snow pits. However, a few issues can be identified with this data:

- *Wetness is reported in only a few classes, that span a wide range of liquid water content. For example, following the international classification (see Fierz et al. (2009)), wetness class 3 spans 3-8% LWC.*
- *Judging wetness of the snowpack is generally difficult and has a subjective component. From our own experience (not published), we did see discrepancies between snow wetness reported by observers, and measurements by Denoth, SnowFork or upGPR.*
- *Manual snow profiling is generally done in the morning hours, thus before the onset of snow melt. Generally, no repeat snow profiles are made during the day to follow the changes in LWC distribution during the day. In contrast, bulk LWC derived from upGPR is able to follow diurnal cycles and a comparison with SNOWPACK simulations have been made (see Heilig et al. (2015)), showing a relatively good correspondence between simulated and observed bulk LWC. However, it is not (yet) possible to derive the vertical spatial distribution inside the snowpack from the radar signal.*

In Figure 1, an example is shown of the LWC distribution as simulated, together with the LWC reported by the observers. Although observers may report 5 wetness classes, we decided to only show data in three classes (0% LWC (dry), 0-3% LWC (mois) and $\geq 3\%$ LWC (wet)) because of the aforementioned reasons. We will add this data in all the figures in the manuscript and supplement when revising.

P20 L8 NSE coefficient of snow-height driven simulation is better. I agree accurate percolation time is one of the reasons of it. In addition to this, does the difference of date of snow disappearance affect NSE? In many years, snow disappeared faster in precipitation driven simulation than that in snow-height driven simulation. In NSE estimation, did you consider the period after snow disappearance in precipitation driven simulation? Also, Table 1 had better include difference of date of snow disappearance.

This is an interesting question. In order to test the sensitivity of the NSE coefficients to the period chosen, we calculated the coefficients in two ways: either taking the melt-out date from the measured snow height or from the simulated snow height (both defined as less than 5 cm of snow remaining). The latter approach was used to calculate the values in the table. On the average NSE coefficients for the studied period, this has not a large impact (typically influencing average NSE coefficients by less than 0.01). However, in individual years, differences may be larger (up to 0.16), in particular for precipitation driven simulations. For this simulation type, the melt out dates are not as well predicted as for the snow height driven type. Nevertheless, the differences between simulation setups within either snow height driven simulations or precipitation driven ones are smaller than the differences between both simulation types. This implies that the same conclusions can be drawn, regardless of the choice of calculation period.

The influence on r^2 values is larger, due to the fact that the last days of melt out are often associated with large snowpack runoff. We will introduce a section in the manuscript discussing the effects of the choice of calculation period. Following the reviewers' suggestion, we added the difference in melt out date in the table, which will help interpreting these results (see Table 1 in

this document). Note that this table contains slightly different values for NSE and r^2 compared to the original manuscript, as there were a few discrepancies how it was determined which period should be analysed. They were revealed when performing the analysis as recommended by the reviewer. Furthermore, we have to apologize for reporting correlation coefficients (r) instead of the coefficients of determination (r^2) for cold contents, isothermal part and avg. grain size, although the table suggested otherwise. This is also corrected now.

P20 L16 In Fig6a, different Y-axes were used for different depth of sensor of soil temperature. Before I aware the difference of y-axis, soil temperature seemed to be stable around 3 and 6 degree Celsius at 30cm and 50 cm in depth, respectively. To avoid misunderstand, caption is necessary at the right side, and scales of right side should show 0 at the zero-point.

We changed the figure as suggested by the reviewer (see Figure 2 in this document). We are sorry to have caused confusion here.

P22L3 Is Figure 8a misdescription of Figure8? Also, It needs caption on right side and showing 0 at the zero-point as well as previous comment for Fig. 6.

Figure 8a should indeed be Figure 8. We changed this figure also as suggested by the reviewer, which entail similar changes as shown in Figure 2 in this document. We are sorry to have caused confusion here.

P24 L1 Fig. 11 showed comparison of measured and simulated snow density separating upper, middle and lower part. I think it is suitable using relative height (1 at the top and 0 at the bottom) like relative date used in Fig. 2, and compare at the specific relative heights (e.g. 0.1, 0.5 and 0.9).

We changed the figure as proposed by the reviewer, showing the snow density in the lower part (0-25% of snow height), the middle part (37.5%-62.5% of snow height) and the upper part (75%-100% of snow height) of the snowpack. See Figure 3 in this document. We did not scale the time axis between 0 and 1 for the beginning and end of the snow season respectively, as snow density is not a continuous measurement, but only a biweekly one. That means that there are typically 12-16 snow profiles per snow season, and scaling these between 0 and 1 is in our opinion not improving the figure as the time resolution is too low. As we do not think this figure is conveying a clearer message than the one in the manuscript, we do not plan to make a change here.

P25 L7 According to fig. 13a, simulated increase of average grain size during melt season seems to be smaller than that in observation. Also, according to fig. 13b, simulated SD was smaller than observed SD. Although display of average and SD express overall trend, it is not easy to find the reason of discrepancies. Can you add the example of direct comparison of grain size profile in supplement figures?

Similar to liquid water content, we will add the biweekly profile data for grain size now in the figures, as shown, by way of example, in Figure 4 in this document.

P21 L11 and P27 L26 Isothermal part of snow temperature relates the wet snow area. In terms of isothermal part of temperature, simulation result of RE scheme corresponded better with ob-

servations than bucket scheme. On the other hand, comparing with the upGPR measurement, bucket scheme corresponded better with observation. Can you explain the reason of this contradict results?

The contradictory result is in our opinion a consequence of the short period of upGPR data (only 4 snow seasons), compared to the full period of 15 years used for determining the statistics. Furthermore, the statistics are determined for all snow profiles, also those made in the beginning of the snow season (October and November), where regularly snow melt is occurring. See for example Figures S3a,b,g,h and S4i,j, and S5c,d,g,h in the Supplement. As this comment points us to the importance of having grain type information in the manuscript, we will include the grain types from the simulations and the observed profiles in the online Supplement for completeness. We originally did not plan to extensively discuss grain type evolution by the model, as the manuscript is already quite long. Furthermore, grain types from the SNOWPACK model can be regarded as a post-processing of the microstructural parameters in the model, whereas the other variables discussed in the manuscript are explicitly evaluated in the simulations.

P29 L19 In conclusion, you wrote "updated soil module can provide a correct lower boundary for snowpack in the model". Is it written in the main text? I could not find the discussion of difference of reproducibility at the boundary with calculation schemes in section 4.3 and Figure 6b.

It is true that it was not explicitly stated in section 4.3. We will amend the sentence on p. 2674, L27 as:

Figure 6b shows that the simulations capture the variability in early season soil-snow interface temperature to a high degree in most years and that the soil module in SNOWPACK is providing an accurate lower boundary for the snow cover in simulations.

References

- Fierz, C., R. Armstrong, Y. Durand, P. Etchevers, E. Greene, D. McClung, K. Nishimura, P. Satyawali, and S. Sokratov (2009), The International Classification for Seasonal Snow on the Ground (ICSSG), *Tech. rep.*, IHP-VII Technical Documents in Hydrology No. 83, IACS Contribution No. 1, UNESCO-IHP, Paris.
- Heilig, A., C. Mitterer, L. Schmid, N. Wever, J. Schweizer, H.-P. Marshall, and O. Eisen (2015), Seasonal and diurnal cycles of liquid water in snow - Measurements and modeling, *J. Geophys. Res.*, doi:10.1002/2015JF003593, accepted.
- Hirashima, H., S. Yamaguchi, and T. Katsushima (2014), A multi-dimensional water transport model to reproduce preferential flow in the snowpack, *Cold Reg. Sci. Technol.*, 108, 80–90, doi:10.1016/j.coldregions.2014.09.004.
- Katsushima, T., S. Yamaguchi, T. Kumakura, and A. Sato (2013), Experimental analysis of preferential flow in dry snowpack, *Cold Reg. Sci. Technol.*, 85, 206–216, doi:10.1016/j.coldregions.2012.09.012.
- Proksch, M., N. Rutter, C. Fierz, and M. Schneebeli (2015), Intercomparison of snow density measurements: bias, precision and spatial resolution, *Cryosphere Discuss.*, 9(4), 3581–3616, doi:10.5194/tcd-9-3581-2015.
- Schlögl, S., R. Mott, and M. Lehning (2015), Assessment of turbulent flux parametrizations over snow using different stability corrections, in *IUGG General Assembly*.

Yamaguchi, S., T. Katsushima, A. Sato, and T. Kumakura (2010), Water retention curve of snow with different grain sizes, *Cold Reg. Sci. Technol.*, 64(2), 87 – 93, doi: 10.1016/j.coldregions.2010.05.008.

Yamaguchi, S., K. Watanabe, T. Katsushima, A. Sato, and T. Kumakura (2012), Dependence of the water retention curve of snow on snow characteristics, *Ann. Glaciol.*, 53(61), 6–12, doi: 10.3189/2012AoG61A001.

Table 1: Average and standard deviation (in brackets) of bulk snowpack statistics over all snow seasons for various simulation setups (bucket or Richards equation (RE) water transport scheme, snow height (HS) or precipitation (Precip) driven simulations, Y2010 (*Yamaguchi et al., 2010*) or Y2012 (*Yamaguchi et al., 2012*) water retention curves, and arithmetic or geometric mean for hydraulic conductivity) for all simulated snow seasons. Differences are calculated as modelled value minus measured value, ratios are calculated as modelled value divided by measured value. The isothermal part is only considered during the melt phase (from March to the end of the snow season).

Variable	Bucket	HS driven (2000-2014)			Precip driven (1997-2014)	
		RE-Y2010AM	RE-Y2012AM	RE-Y2012GM	Bucket	RE-Y2012AM
RMSE HS (cm)	4.16 (1.73)	4.00 (1.56)	4.11 (1.64)	4.12 (1.71)	20.86 (12.31)	23.12 (11.38)
Difference HS (cm)	1.33 (2.24)	0.87 (2.09)	0.88 (2.17)	0.89 (2.21)	-1.23 (12.31)	-5.24 (11.38)
Difference melt out (days)	-0.67 (1.45)	-0.73 (1.44)	-0.73 (1.44)	-0.73 (1.44)	-3.94 (6.08)	-7.00 (6.83)
RMSE SWE (mm w.e.)	39.28 (15.51)	39.62 (14.71)	39.78 (15.50)	39.39 (15.45)	84.96 (36.34)	99.03 (36.23)
Difference SWE (mm w.e.)	-5.67 (27.20)	-7.08 (27.04)	-9.29 (27.05)	-8.06 (27.14)	-16.14 (67.61)	-36.00 (66.91)
Ratio SWE (mm w.e.)	1.01 (0.09)	0.99 (0.08)	0.99 (0.08)	0.99 (0.08)	0.97 (0.19)	0.91 (0.17)
Ratio runoff sum (-)	1.08 (0.28)	1.14 (0.28)	1.13 (0.28)	1.13 (0.28)	0.98 (0.31)	0.98 (0.31)
NSE 24 hours (-)	0.72 (0.32)	0.73 (0.32)	0.73 (0.32)	0.73 (0.32)	0.66 (0.32)	0.67 (0.31)
NSE 1 hour (-)	0.13 (0.37)	0.57 (0.35)	0.59 (0.34)	0.58 (0.34)	0.02 (0.39)	0.39 (0.34)
r^2 24 hrs runoff sum (-)	0.85 (0.11)	0.87 (0.10)	0.87 (0.10)	0.87 (0.10)	0.84 (0.12)	0.85 (0.13)
r^2 1 hour runoff sum (-)	0.52 (0.06)	0.78 (0.08)	0.78 (0.08)	0.78 (0.08)	0.48 (0.07)	0.68 (0.11)
Lag correlation for runoff (h)	-1.47 (0.79)	-0.20 (0.37)	-0.17 (0.31)	-0.13 (0.30)	-1.72 (0.79)	-0.44 (0.48)
RMSE cold contents (kJ m ⁻²)	627 (274)	529 (244)	554 (285)	551 (277)	786 (556)	742 (509)
Difference cold contents (kJ m ⁻²)	-129.0 (312.9)	11.1 (326.2)	-30.5 (336.2)	-36.7 (322.9)	-46.0 (604.0)	62.4 (565.0)
r^2 cold contents (-)	0.76 (0.36)	0.78 (0.36)	0.79 (0.36)	0.78 (0.36)	0.77 (0.36)	0.78 (0.36)
r^2 isothermal part (-)	0.64 (0.33)	0.74 (0.36)	0.74 (0.36)	0.73 (0.35)	0.65 (0.32)	0.74 (0.36)
r^2 avg. grain size (-)	0.47 (0.31)	0.45 (0.30)	0.45 (0.30)	0.45 (0.30)	0.39 (0.29)	0.37 (0.28)
Mass balance error (mm w.e.)	0.01 (0.00)	0.01 (0.00)	0.01 (0.00)	0.01 (0.00)	0.09 (0.25)	0.02 (0.03)
Energy balance error (W m ⁻²)	0.03 (0.08)	0.06 (0.08)	0.06 (0.08)	0.05 (0.08)	-0.05 (0.07)	0.05 (0.08)
CPU time (min)	0.57 (0.07)	1.39 (0.26)	1.44 (0.36)	1.45 (0.37)	0.61 (0.11)	1.55 (0.45)

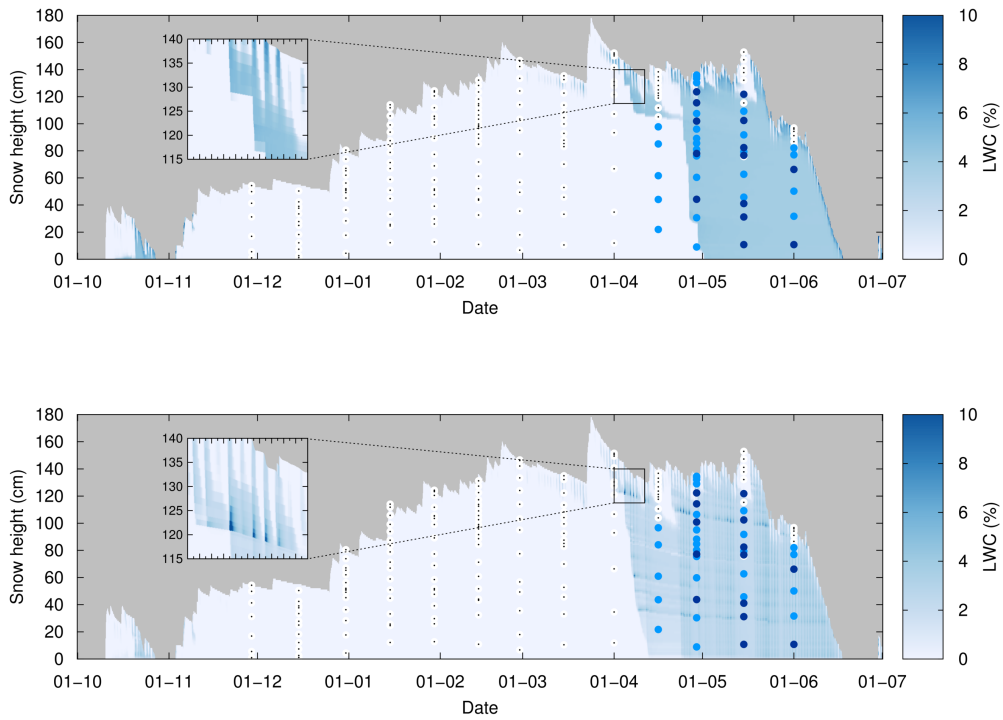


Figure 1: Snow LWC (%) for the snow height-driven simulation with the bucket scheme (a) and with Richards equation using the *Yamaguchi et al.* (2012) water retention curve and arithmetic mean for hydraulic conductivity (RE-Y2012AM, (b)), for the example snow season 2014. Dots denote layers that have been reported as dry (0% LWC, white with black center dot), moist (0-3% LWC, light blue) or wet, very wet or soaked ($\geq 3\%$ LWC, dark blue) from the biweekly snow profiles. When layers are reported as "1-2" (dry-moist), it is considered moist. In the zoom insert, major and minor x-axis ticks denote midnight and noon, respectively.

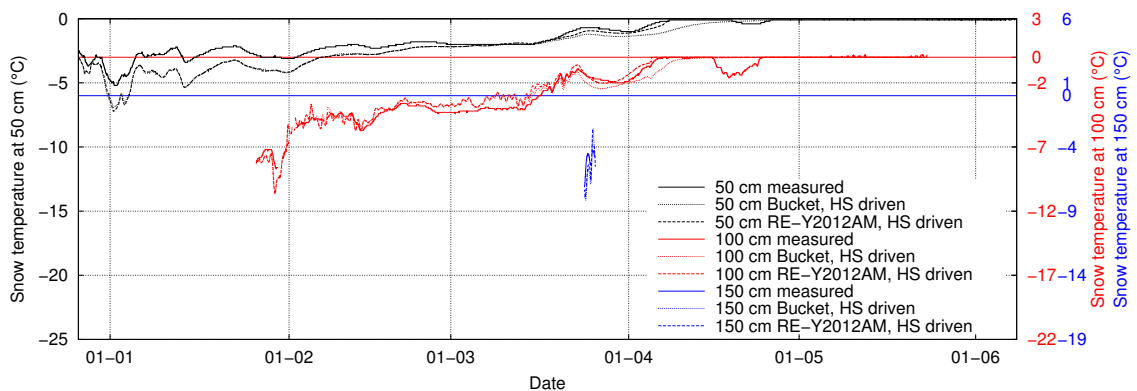


Figure 2: Measured and modelled snow temperatures at 50, 100 and 150 cm above the ground for snow height-driven (HS driven) simulations using the bucket scheme or Richards equation using the *Yamaguchi et al.* (2012) water retention curve and arithmetic mean for hydraulic conductivity (RE-Y2012AM) for the example snow season 2014. Values are only plotted when the snow height was at least 20 cm more than the height of the temperature sensor. Note that the x-axes for 100 and 150 cm depth are staggered by 3 °C to prevent overlap.

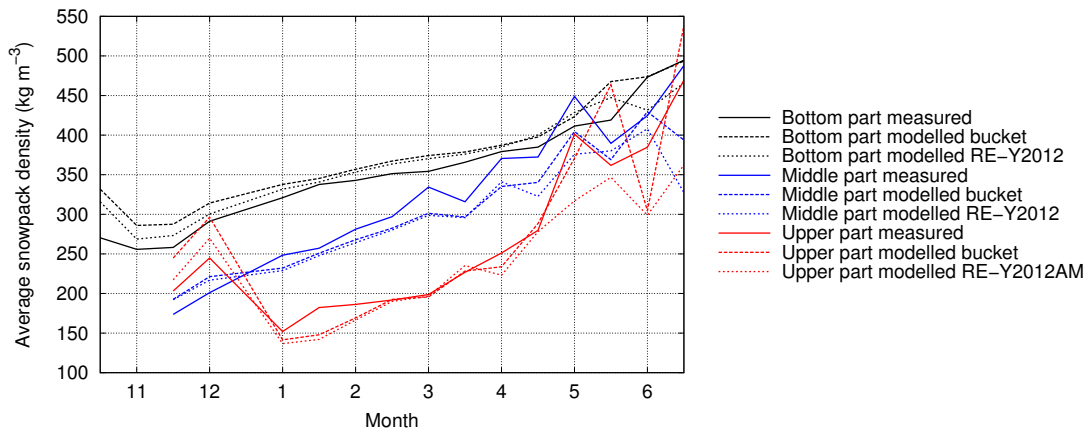


Figure 3: Average simulated and measured snow density (kg m^{-3}) for the relative lower (0 – 25 %), middle (37.5 – 52.5 %) and upper part (75 – 100 %) of the snowpack height.

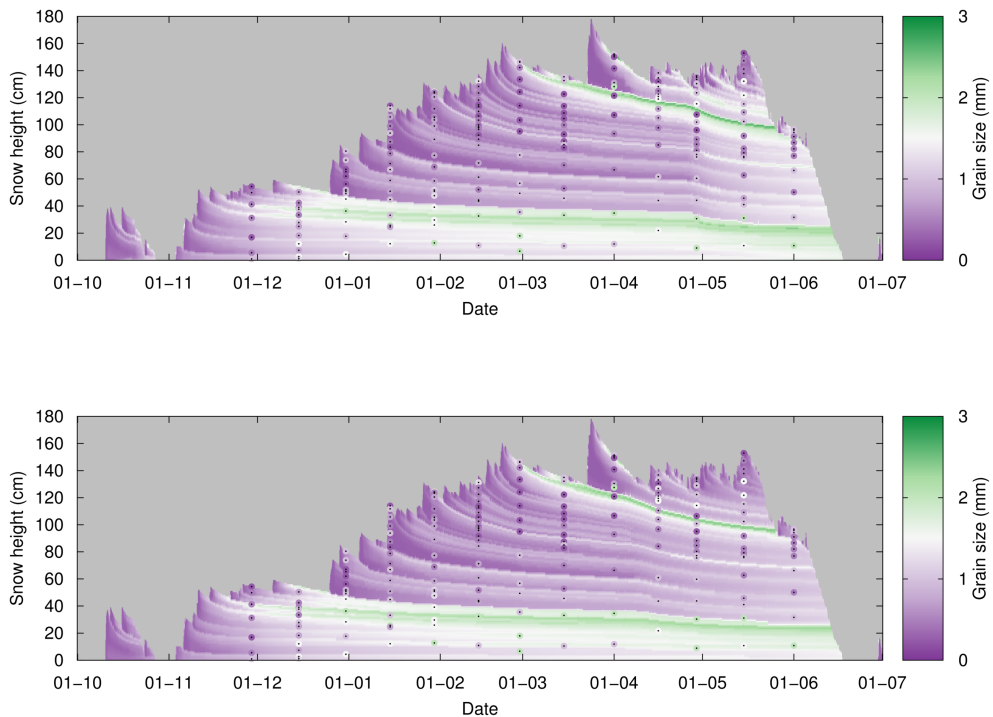


Figure 4: Grain size (mm) for the snow height-driven simulation with the bucket scheme (**a**) and with Richards equation using the *Yamaguchi et al.* (2012) water retention curve and arithmetic mean for hydraulic conductivity (RE-Y2012AM, **b**), for the example snow season 2014. Dots with a black center point indicate observed grain sizes reported from the biweekly snow profiles, where the black center point is located in the middle of the observed layer.

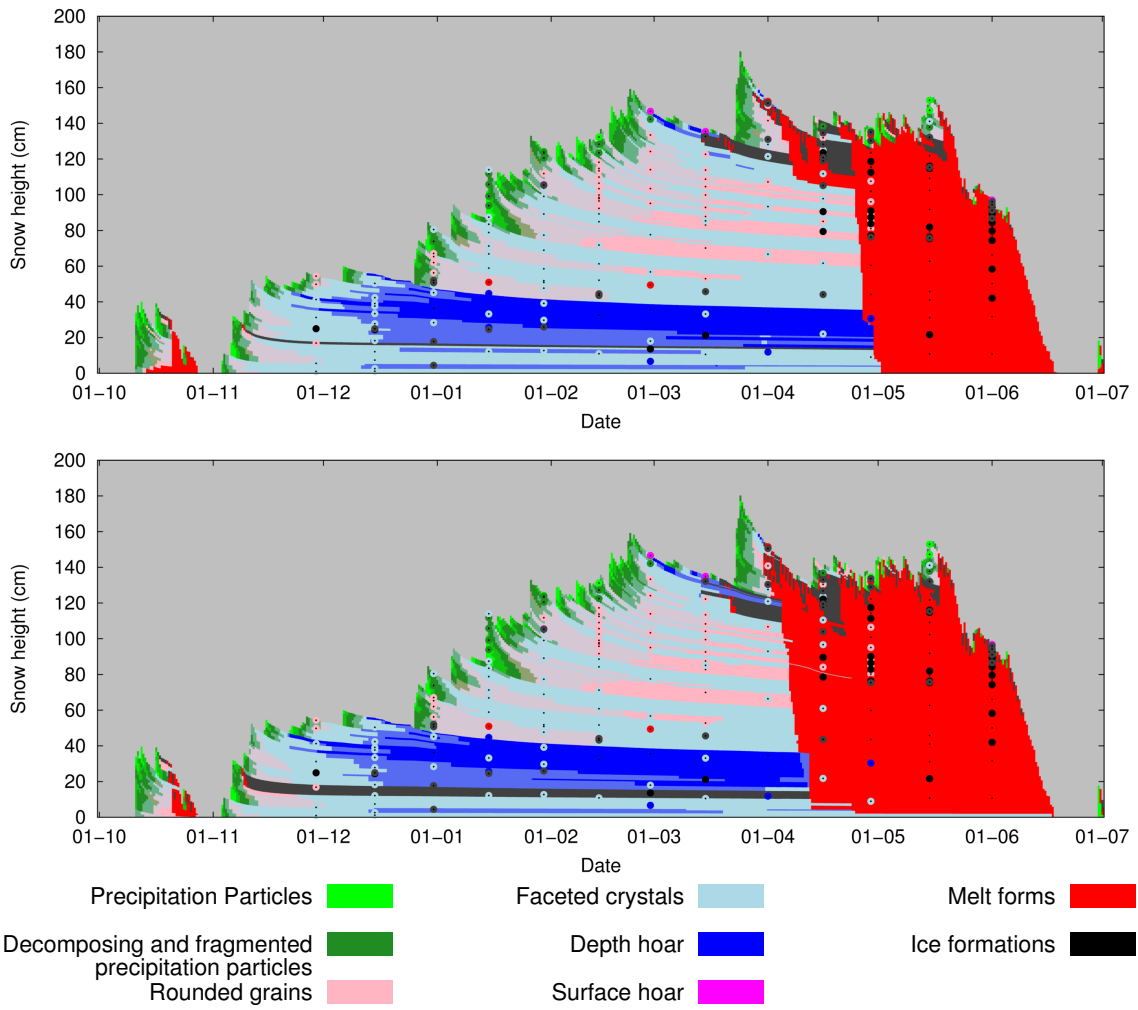


Figure 5: Grain type for the snow height-driven simulation with the bucket scheme **(a)** and with Richards equation using the *Yamaguchi et al. (2012)* water retention curve and arithmetic mean for hydraulic conductivity (RE-Y2012AM, **(b)**), for the example snow season 2014. Dots with a black center point indicate observed grain types reported from the biweekly snow profiles, where the black center point is located in the middle of the observed layer.

Reviewer 2

This work is remarkable at least from three points of view: for the abundance of reliable data used (and unfortunately not provided to the public of researchers), the use of modern parameterisations of the snowpack evolution, using a new version of SNOWPACK 1d model which includes water flux moved by Richards equation and a new parameterisation of soil temperature, and, last but not least, the trial to get quantitative answer without parameters' calibration. The report of the results is detailed and honest. Some results, as stated by the same Authors, seem to be a byproduct of SNOWPACK being 1D, and this should probably discussed at a deeper level. Information about the SNOWPACK model availability and data availability are required, maybe in Acknowledgements or in a short dedicated section (entailed for instance: How to Replicate this Research). Future work could address the reliability of parameters and their sensitivity estimation. It seems clear to me, in fact, that some a-priori, parameterisations could not be the correct: indeed, a little qualitative discussion on these topics could be interesting also in this paper.

Overall the paper is excellent and worth to be published in TC, after some minor revision work. Please find below my detailed observations.

We would like to thank the reviewer for the positive feedback and the constructive comments. Regarding the parameters used in the SNOWPACK model: they mostly have been published before, as indicated by the references provided in the manuscript. We think it is interesting to combine a short discussion on possible future improvements of process representations in the outlook section, which was proposed by the first reviewer. We will discuss this on a process level, rather than a parameter level, because snow settling, for example, depends on several parameters and we think that it would be too detailed in the context of the manuscript to discuss individual parameters.

Please find our detailed response to the other issues raised by the reviewer below.

Detailed comments

Page 2659 - Introduction is well designed. Probably a short of literary review about model alternatives to SNOWPACK would help the general reader to have a more clear view of possibilities.

We will mention alternative models in the introduction, restricted to the multi-layer physics based models SNTHERM, CROCUS and SNOWPACK:

One-dimensional multi-layer physics based snowpack models, as for example SNTHERM89 (Jordan, 1991), CROCUS (Brun et al., 1989; Vionnet et al., 2012) and SNOWPACK (Lehning et al., 2002a,b) are widely used to assess various aspects of the snow cover.

Page 2664 - The data collection is impressive. More information about data availability, needed.

It has been decided now that the operational data from WFJ (both the meteorological forcing, the snow lysimeter data as well as the biweekly snow profiles) will be made available on a repository with the publication of this manuscript, linked via DOIs. The SNOWPACK model is available under the GNU Lesser General Public License (LGPL) Version 3; we will include a link to the repository (<http://models.slf.ch>) in the revised manuscript. The data from the upward-looking ground penetrating radar in combination with snow profiles made in its vicinity, has been collected on a project-basis and is available on request from the authors. We will add this information in the Acknowledgements.

Page 2665 - Since the way SNOWPACK is initialised has strong impact on the results, a little more of explanation on how HS approach works, as opposed to Precept driven, could be useful.

Although the algorithm has already been described in Lehning et al. (1999), we agree with the reviewer that due to the importance of the snow height driven approach in the manuscript, it is helpful to expand on the approach. Basically, if the measured snow height exceeds the modelled one, the model will create as many layers of 2 cm as necessary to match the observed snow height again, if snowfall conditions are met. The snowfall conditions are: (i) measured air temperature ≤ 1.2 °C, (ii) difference between measured air temperature and modelled snow temperature ≤ 3.0 °C and (iii) a relative humidity ≥ 70 %. These conditions provide an estimation whether the atmospheric conditions are such that snowfall can be expected. For example, the second condition tests for cloudy conditions, when the increase in incoming longwave radiation compared to cloud-free conditions will cause the snow surface temperature to increase and become close to the air temperature. We will provide this information in the manuscript.

Page 2673 - line 22 - I think this is an improper use of the supplement. Figure S8 should be added to the main text. (What is IMO an appropriate use of the Supplement is shown in lines 2-3 of page 2675).

We understand that it is necessary to show Figure S8 in the main text. We will make this change in the revised manuscript.

Page 2674 - line 8 - The discussion about the NSE coefficients found should be more extensive. While most of them are good, some of the coefficient are really bad (NSE 1h bucket). Therefore, these performance should be discussed. I agree that NSE could not be the best test: but, in case, this also should be discussed.

To prevent being biased towards performance in terms of NSE coefficients, we also included r^2 statistics. Originally we decided not to discuss the results regarding runoff in too much detail, as this would then be a repetition of our previous work (Wever et al., 2014). The main problem with the performance of the bucket scheme on hourly time scales when looking at NSE coefficients is poor timing due to neglecting the travel time through the snowpack in the bucket scheme. We will add this in the manuscript, although we still think it is not necessary to provide an extensive discussion as the reference to the other paper is sufficient, in our opinion.

Page 2675 - line 13. "The latter influences the snow temperature through the thermal inertia of dense snow layers and through the strong dependence of density on thermal conductivity (e.g., Calonne et al., 2011). " I was tempted to say that is the thermal conductivity that depends upon the density, not vice-versa.

We are sorry to have caused confusion here, but it is indeed intended to say that the thermal conductivity is dependent on density. We revised this sentence as:

The latter influences the snow temperature through the thermal inertia of dense snow layers and through the strong density dependence of thermal conductivity (e.g., Calonne et al., 2011).

Page 2676 - line 25. p.2676: "The contrasting result suggests that the snow layers near the top of the snowpack have a too low density in the simulations." Why not incorrect estimation of incoming solar radiation ? Or of the thermal capacity, for reasons not depending on density ? I am not able to grasp the reasons for the unique interpretations the Authors give for this behaviour.

We agree that more explanation is required here. We add the possibility that it is not necessarily snow density, which influences thermal conductivity of the snowpack, but that snow density errors also introduce errors in thermal capacity. We will add that a closer inspection of the simulations revealed that the underestimation of snow surface temperature particularly happens at night (not shown in the paper), which excludes the possible influence of errors in diagnosing the net shortwave radiation. We will revise the text as follows:

"Interestingly the snow surface temperature is generally underestimated, whereas the temperature at the highest snow temperature sensor is overestimated in the simulations. The contrasting result suggests that the snow layers near the top of the snowpack have a too low density in the simulations, impacting both thermal conductivity and heat capacity of those layers, or the thermal conductivity is underestimated for typical snow densities found close to the surface. These effects provide a stronger isolation of the snowpack, causing heat from inside to escape at a slower rate and allowing the surface to cool more. This offers an explanation why the underestimation of the snow surface temperature particularly occurs at night (not shown). In contrast, errors in diagnosing the snowpack energy balance (i.e., in net shortwave or longwave radiation, or turbulent fluxes) would be expected to influence all temperature sensors in the same direction."

Page 2677 - line 13 and subsequents. ". . . suggesting a better timing of the movement of the meltwater front through the snowpack ..". How this is actually affected by the fact that SNOWPACK is 1D ? Is this a manifestation of 3D effects of water re-distribution ?

It is indeed true that the fact that SNOWPACK is only 1D, and assuming horizontal homogeneity is a simplification of reality that will be particularly important for simulating liquid water flow. We think this issue is clearly illustrated by the fact that although the timing of the movement of the meltwater front through the snowpack is improved, the runoff as measured by the snow lysimeter consistently starts earlier than simulated. To better reflect that the snow temperature may also rise to 0°C by heat advection or refreezing of liquid water infiltrating the layer, the section will be rewritten as:

"Although this suggests a better timing of the movement of the meltwater front through the snowpack and the associated temperature increase to 0°C, also heat advection through the ice matrix and preferential flow and subsequent refreezing inside the snowpack may increase the local snowpack temperature to 0°C. The reason why the results from the temperature series at 150 cm contrast those at 0, 50 and 100 cm depth remains unclear."

Page 2694 - Figure 1 - The Figure is actually not very clear because some lines superimpose. Maybe this can be explained in the caption.

We will add in the caption that apart from forcing with either snow height or precipitation measurements, differences between simulation setups cause only small differences in snow height simulations, resulting in overlapping lines in the figure.

Page 2695 - Figure 2. This Figure is very explicative respect to the quality of the drivers. Maybe some more explanation can be added to comment it in the text. The difference between the two drivers seems related to the SD and both of them seems to have close to null bias. However Precip driven simulations show strong seasonality with positive difference in the central months. Why ?

The snow height driven simulations are forced to closely follow the measured snow height, and overestimations in snow melt or snow settling can be compensated for, which explains good agreement. The precipitation driven simulations on the other hand, rely solely on measured precipitation. The seasonality in the difference with measured snow height stems from the fact that SNOWPACK seems to overestimate snow melt for WFJ, leading to an overestimated SWE depletion in spring. However, during the accumulation phase, it seems that particularly a few large snowfall events are overestimated by the rain gauge measurements, including undercatch correction (see Figure S2e in the Supplement for winter season 2011-2012 for a very illustrative example), whereas for typical snowfall events, the undercatch correction works well. Once events are overestimated, it will continue to bias the difference of simulated and measured snow height, as there is no mechanism to compensate for the error, in contrast with the snow height measurements. We will provide some more explanation regarding these issues in the text.

Page 2696 - Page 2697 - Figure 3 and 4 have mm in ordinate. Using cm would be homogeneous with the rest of the paper.

Although it is true that this seems an inconsistency, we prefer to keep the original notation, as it is very common in literature to express snow height in cm, and SWE in mm w.e.

Page 2698 - Figure 5 - The RE plot shows sharp variations of LWC on the vertical that move downward in time. This is fine with me. However, we also observe jumps in liquid water content from instant to instant. Are these jumps instantaneous just for representation problems or there are more detailed dynamics ?

These jumps are associated with the diurnal variation in LWC, as we explained on p2672, L24-26 and p6-7. We found correspondence of modelled diurnal variations using RE with those derived from field measurements using the upGPR (Heilig et al., 2015). As the figures are probably too small to convey these temporal and spatial variations, and to better illustrate the difference between the bucket scheme and RE, we have put a detail from the simulations inside the figures, see Figure 1 in this document.

Page 2702 - Figure 9b. Please use SD for Standard deviation instead of S.D.

We will adjust the figures accordingly.

Page 2703 - Same comment as in Figure 5

Please see my response there, considering the fact that snow density is also influenced by variations in water content and thereby can exhibit diurnal variations.

Page 2705 - Figure 132 - Grain size: does grain of relative large size move downwards due to compaction ? (Or there is also a metamorphism associated ?) Therefore does also liquid water content (in Figure 5b) move downward due to compaction ? (The same for density ?) Could, please clarify these aspects to me ?

Both processes play a role. First of all, the snowpack is constantly settling due to compaction and overload by snow falls. Furthermore, SNOWPACK considers observed enhanced settling with wetting of the snowpack. Grain size eventually evolves due to metamorphism processes and under the presence of liquid water. The implementation of these processes is detailed in the original SNOWPACK paper by Lehning et al. (2002a). As layers are moving closer to the ground due to settling, the properties keep attached to the layer in the simulations. We think this is an appropriate representation of reality. For this reason, liquid water accumulations inside the snowpack also move downward (as depicted in Figure 5b), although this is not a result of water flow. A note is added to the manuscript to briefly explain this behaviour:

These accumulations peak at around 10% LWC and occur during the first wetting of the snowpack and above capillary barriers inside the snowpack. The apparent slow downward movement of liquid water accumulations during the melt season results from snowpack settling, moving the specific layers with water accumulations closer to the ground.

Page 2707 - Figure 14. All the 14s figures are indeed interesting. However, putting all of them in the same page produces a quite unreadable result. There is certain complexity in these plots that should be probably better explained. It is true that page 2680 is dedicated to this Figure. However, the connection between the assertions in the text and what represented is not so clear to me.

We are a bit in doubt here what to do. On the one hand, we agree that putting all four figures on one page makes the page rather crowded. On the other hand, we think it is very illustrative to be able to compare the figures directly to each other, which is impossible when the figures are spread over several pages. In the final format, the figures can probably be enlarged when they are printed vertically below each other on two sheets of A4 paper. Another option may be to show the figures in landscape mode. We will discuss this with the typesetting department. Additionally, we labelled the four main observations mentioned on p2680, L28 to P2681, L7 with (i), (ii), (iii) and (iv), and reference them later in the text. We hope that this approach offers more clarity. The revised text:

From the four snow seasons presented in Fig. 14, the following observations can be made: (i) snowpack runoff measured by the snow lysimeter consistently starts earliest in the snow season. (ii) The progress of the meltwater front is always faster in the simulations with RE, compared to the bucket scheme. (iii) The radar-derived meltwater front progresses generally slower through the snowpack than in both water transport schemes in the model. (iv) The manual snow profiles mostly show melt forms in parts of the snowpack that have been wet according to the radar data, whereas the simulations often show larger parts of the snowpack becoming wet earlier than indicated by the profiles. These observations will now be discussed in more detail.

(i) Since preferential flow can route liquid water efficiently through the snowpack (Kattelmann, 1985; Waldner et al., 2004; Techel and Pielmeier, 2011), upGPR-determined depths of dry-wet transitions are not necessarily linked to the onset of measured snowpack runoff (Heilig et al., 2015). Studies by Katsushima et al. (2013) and Hirashima et al. (2014) found that ponding plays a crucial role in forming preferential flow in both laboratory experiments as well as model simulations. The ponding of liquid water in the simulations for WFJ (see Fig. 1) suggests that preferential flow may have developed. The amount of snowpack runoff measured before the arrival of the meltwater front is highly variable. From 1 until 8

April in snow season 2011, large amounts of snowpack runoff were observed, most likely due to lateral flow processes, whereas in snow season 2014, only marginal amounts were observed. In the latter snow season, there is a strong increase in observed snowpack runoff close to the time of the arrival of the radar-derived meltwater front at the snowpack base. This variability between years is not necessarily caused by different preferential flow path structures, but may also result from the limited capturing area of the snow lysimeter (Kattelmann, 2000).

(iii, iv) The vertical distribution of the melt forms in the observed snow profiles may be considered particularly representative for matrix flow and for the four presented years it generally corresponds well with the parts of the snowpack that may be considered wet from the upGPR signal. (ii) As the bucket scheme shows a higher correspondence with the upGPR data than RE, the convenient improvement in the accuracy of simulated snowpack runoff with RE, as found in Wever *et al.* (2014), seems to be partly caused by (unintentionally) mimicking some preferential flow effects. To what extent this is caused by parametrisations of the water retention curve or hydraulic conductivity, or by the specifics of the implementation of RE in SNOWPACK, remains unclear. (ii, iii) Although the bucket scheme may seem to better coincide with the meltwater front in the upGPR data, it may as well be argued that the differences between both water transport schemes are smaller than the discrepancies with the upGPR data. It is likely that the limits of one-dimensional models with a single water transport mechanism will prevent a correct simulation of both snowpack runoff as well as the internal snowpack structure at the same time.

In the beginning of the melt season, observations contrasting to the main melt phase discussed above can be made. The initial melt phase is characterized by a regularly disappearing meltwater front at night. In this period, the depth to which the liquid water infiltrates the snowpack is underestimated in the simulations. Here, the RE scheme shows larger infiltration depths, which are in better agreement with the upGPR data, although again differences between both simulations are smaller than the discrepancies with the upGPR data. This result is contradictory with the main melt phase, where the speed with which the meltwater front progresses through the snowpack is largely overestimated in the simulations. Furthermore, the distribution of melt forms in the snow profiles does not always coincide with the deeper infiltration depths detected by the upGPR.

References

- Brun, E., E. Martin, V. Simon, C. Gendre, and C. Coléou (1989), An energy and mass model of snow cover suitable for operational avalanche forecasting, *J. Glaciol.*, 35(121), 333–342.
- Heilig, A., C. Mitterer, L. Schmid, N. Wever, J. Schweizer, H.-P. Marshall, and O. Eisen (2015), Seasonal and diurnal cycles of liquid water in snow - Measurements and modeling, *J. Geophys. Res.*, doi:10.1002/2015JF003593, accepted.
- Hirashima, H., S. Yamaguchi, and T. Katsushima (2014), A multi-dimensional water transport model to reproduce preferential flow in the snowpack, *Cold Reg. Sci. Technol.*, 108, 80–90, doi:10.1016/j.coldregions.2014.09.004.
- Jordan, R. (1991), A one-dimensional temperature model for a snow cover: Technical documentation SN THERM.89, *Tech. Rep. Spec. Rep. 657*, U.S. Army Cold Reg. Res. Eng. Lab., Hanover, NH.
- Katsushima, T., S. Yamaguchi, T. Kumakura, and A. Sato (2013), Experimental analysis of preferential flow in dry snowpack, *Cold Reg. Sci. Technol.*, 85, 206–216, doi:10.1016/j.coldregions.2012.09.012.
- Kattelmann, R. (1985), Macropores in snowpacks of Sierra Nevada, *Ann. Glaciol.*, 6, 272–273.
- Kattelmann, R. (2000), Snowmelt lysimeters in the evaluation of snowmelt models, *Ann. Glaciol.*, 31(1), 406–410, doi:10.3189/172756400781820048.

- Lehning, M., P. Bartelt, B. Brown, T. Russi, U. Stöckli, and M. Zimmerli (1999), SNOWPACK calculations for avalanche warning based upon a new network of weather and snow stations, *Cold Reg. Sci. Technol.*, 30(1–3), 145–157, doi:10.1016/S0165-232X(99)00022-1.
- Lehning, M., P. Bartelt, B. Brown, C. Fierz, and P. Satyawali (2002a), A physical SNOWPACK model for the Swiss avalanche warning Part II: Snow microstructure, *Cold Reg. Sci. Technol.*, 35(3), 147–167, doi:10.1016/S0165-232X(02)00073-3.
- Lehning, M., P. Bartelt, B. Brown, and C. Fierz (2002b), A physical SNOWPACK model for the Swiss avalanche warning Part III: Meteorological forcing, thin layer formation and evaluation, *Cold Reg. Sci. Technol.*, 35(3), 169–184, doi:10.1016/S0165-232X(02)00072-1.
- Techel, F., and C. Pielmeier (2011), Point observations of liquid water content in wet snow – investigating methodical, spatial and temporal aspects, *Cryosphere*, 5(2), 405–418, doi:10.5194/tc-5-405-2011.
- Vionnet, V., E. Brun, S. Morin, A. Boone, S. Faroux, P. Le Moigne, E. Martin, and J.-M. Willemet (2012), The detailed snowpack scheme Crocus and its implementation in SURFEX v7.2, *Geosci. Model Dev.*, 5(3), 773–791, doi:10.5194/gmd-5-773-2012.
- Waldner, P. A., M. Schneebeli, U. Schultze-Zimmermann, and H. Flüeler (2004), Effect of snow structure on water flow and solute transport, *Hydrol. Proc.*, 18(7), 1271–1290, doi:10.1002/hyp.1401.
- Wever, N., C. Fierz, C. Mitterer, H. Hirashima, and M. Lehning (2014), Solving Richards Equation for snow improves snowpack meltwater runoff estimations in detailed multi-layer snowpack model, *Cryosphere*, 8(1), 257–274, doi:10.5194/tc-8-257-2014.
- Yamaguchi, S., K. Watanabe, T. Katsushima, A. Sato, and T. Kumakura (2012), Dependence of the water retention curve of snow on snow characteristics, *Ann. Glaciol.*, 53(61), 6–12, doi:10.3189/2012AoG61A001.

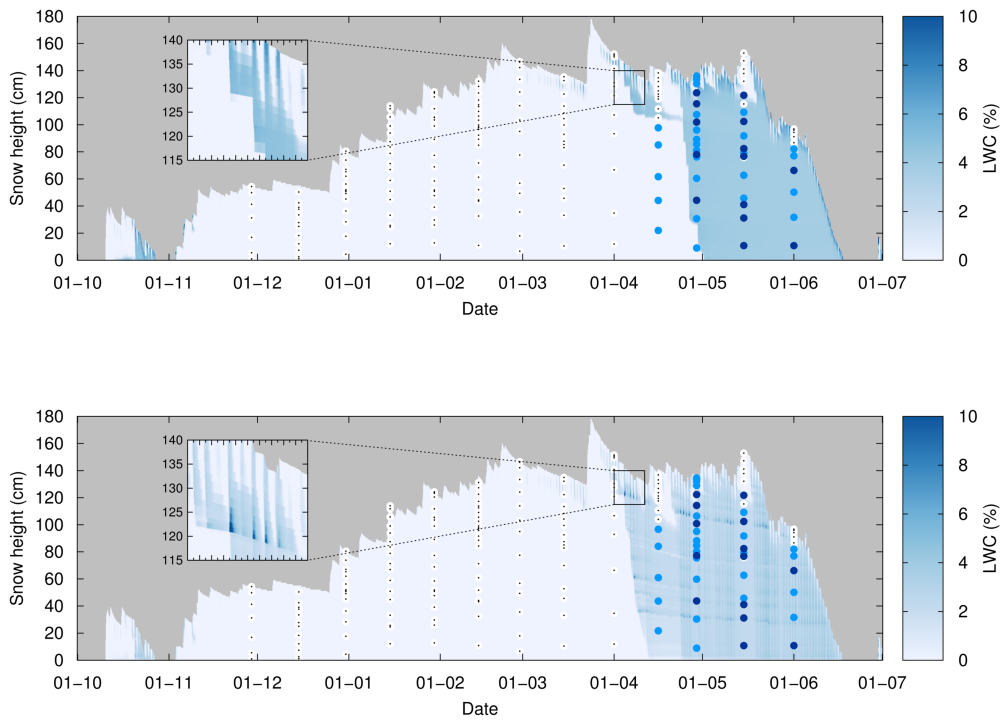


Figure 1: Snow LWC (%) for the snow height-driven simulation with the bucket scheme **(a)** and with Richards equation using the *Yamaguchi et al. (2012)* water retention curve and arithmetic mean for hydraulic conductivity (RE-Y2012AM, **(b)**), for the example snow season 2014. Dots denote layers that have been reported as dry (0% LWC, white with black center dot), moist (0-3% LWC, light blue) or wet, very wet or soaked ($\geq 3\%$ LWC, dark blue) from the biweekly snow profiles. When layers are reported as "1-2" (dry-moist), it is considered moist. In the zoom insert, major and minor x-axis ticks denote midnight and noon, respectively.

Reviewer 3

I have also sent a list of editorial suggestions that are not of interest for the open discussion directly to the authors.

We thank Richard Essery for his helpful comments and corrections, which we will take into account when revising the manuscript.

The site is sometimes abbreviated as "WFJ" and sometimes "the WFJ" - pick one.

We use "WFJ" consistently now.

page 2660: Not much space would be required to quote the Richards Equation and the van Genuchten water retention curve here for the benefit of the general reader.

We will include both in the revised manuscript.

page 2665: If the cylinder is inserted horizontally into the snow, "60 cm long" would be a better description than "high".

The cylinder is inserted vertically. To clarify the text here, we revised it as (a colleague informed us that the cylinder is 55 cm high):

Density is determined by taking snow cores using a 55 cm high aluminium cylinder with a cross-sectional area of 70 cm² inserted vertically into the snowpack. The snow core is then weighted using a calibrated spring.

page 2675: Is "dependence of thermal conductivity on density" intended?

We are sorry to have caused confusion here, but it is indeed intended to say that the thermal conductivity is dependent on density. We revised this sentence as:

The latter influences the snow temperature through the thermal inertia of dense snow layers and through the strong density dependence of thermal conductivity (e.g., Calonne et al., 2011).

Figures 6 and 8: The captions should note that the temperature axes are staggered to avoid overlap. Some of the broken line styles are impossible to distinguish; longer dashes might help.

We will adjust the figures according to the suggestions.

Figure 12: The bucket and RE results look surprisingly similar, with little response to the spring wetting apparent. Is this just due to the colour scale?

We changed the colour scale, in particular to be able to plot the observed grain sizes into the same figure, which required more contrasting colours. This was a suggestion by another reviewer. See Figure 1. Now, by eye it can also be seen that the bucket scheme is associated with larger snow grains in the snow melt season, due to the generally higher LWC compared to the Richards Equation. In the model, the wet snow grain growth rate depends on LWC (Lehning et al., 2002a), based on experimental work by Brun (1989).

References

- Brun, E. (1989), Investigation on wet-snow metamorphism in respect of liquid-water content, *Ann. Glaciol.*, 13, 22–26.
- Lehning, M., P. Bartelt, B. Brown, C. Fierz, and P. Satyawali (2002a), A physical SNOWPACK model for the Swiss avalanche warning Part II: Snow microstructure, *Cold Reg. Sci. Technol.*, 35(3), 147–167, doi:10.1016/S0165-232X(02)00073-3.
- Yamaguchi, S., K. Watanabe, T. Katsushima, A. Sato, and T. Kumakura (2012), Dependence of the water retention curve of snow on snow characteristics, *Ann. Glaciol.*, 53(61), 6–12, doi: 10.3189/2012AoG61A001.

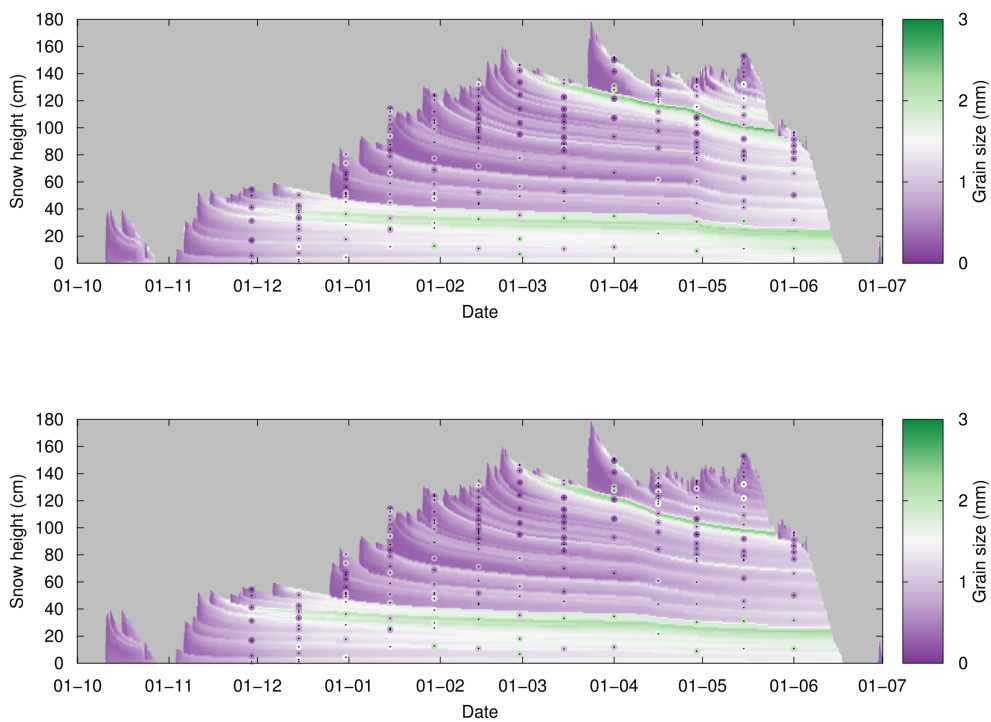


Figure 1: Grain size (mm) for the snow height-driven simulation with the bucket scheme **(a)** and with Richards equation using the *Yamaguchi et al. (2012)* water retention curve and arithmetic mean for hydraulic conductivity (RE-Y2012AM, **(b)**), for the example snow season 2014. Dots with a black center point indicate observed grain sizes reported from the biweekly snow profiles, where the black center point is located in the middle of the observed layer.

Verification of the multi-layer SNOWPACK model with different water transport schemes

N. Wever^{1,2}, **L. Schmid**¹, **A. Heilig**³, **O. Eisen**^{3,4,5}, **C. Fierz**¹, and **M. Lehning**^{1,2}

¹WSL Institute for Snow and Avalanche Research SLF, Flüelastrasse 11,
7260 Davos Dorf, Switzerland

²École Polytechnique Fédérale de Lausanne (EPFL), School of Architecture, Civil and
Environmental Engineering, Lausanne, Switzerland

³Institute of Environmental Physics, University of Heidelberg, Heidelberg, Germany

⁴Alfred Wegener Institute Helmholtz Centre for Polar and Marine Research,
Bremerhaven, Germany

⁵University Bremen, Bremen, Germany

Correspondence to: N. Wever (wever@slf.ch)

Abstract

The widely-used detailed SNOWPACK model has undergone constant development over the years. A notable recent extension is the introduction of a Richards Equation (RE) solver as an alternative for the bucket-type approach for describing water transport in the snow and soil layers. In addition, continuous updates of snow settling and new snow density parametrisations have changed model behaviour. This study presents a detailed evaluation of model performance against a comprehensive multi-year data set from Weissfluhjoch near Davos, Switzerland. The data set is collected by automatic meteorological and snowpack measurements and manual snow profiles. During the main winter season, snow height (RMSE: <math><4.2\text{ cm}</math>), snow water equivalent (SWE, RMSE: <math><40\text{ mm w.e.}</math>), snow temperature distributions (typical deviation with measurements: <math><1.0\text{ }^\circ\text{C}</math>) and snow density (typical deviation with observations: <math><50\text{ kg m}^{-3}</math>) as well as their temporal evolution are well simulated in the model and the influence of the two water transport schemes is small. The RE approach reproduces internal differences over capillary barriers but fails to predict enough grain growth since the growth routines have been calibrated using the bucket scheme in the original SNOWPACK model. ~~The~~ However, the agreement in both density and grain size is sufficient to parametrise the hydraulic properties successfully. In the melt season, ~~more~~ pronounced underestimation of typically 200 mm w.e. in SWE is found. The discrepancies between the simulations and the field data are generally larger than the differences between the two water transport schemes. Nevertheless, the detailed comparison of the internal snowpack structure shows that the timing of internal temperature and water dynamics is adequately and better represented with the new RE approach when compared to the conventional bucket scheme. On the contrary, the progress of the meltwater front in the snowpack as detected by radar and the temporal evolution of the vertical distribution of melt forms in manually observed snow profiles do not support this conclusion. This discrepancy suggests that the implementation of RE partly mimics preferential flow effects.

1 Introduction

~~The one-dimensional~~ One-dimensional multi-layer physics based snowpack ~~model~~ models, as for example SNTHERM89 (Jordan, 1991), CROCUS (Brun et al., 1989; Vionnet et al., 2012) and SNOWPACK (Lehning et al., 2002a, b) ~~has been used in many studies~~ are widely used to assess various aspects of the snow cover. Recently, the SNOWPACK model has been extended with a solver for Richards Equation (RE) in the snowpack and soil, which improved the simulation of liquid water flow in snow from the perspective of snowpack runoff compared to a conventional bucket type approach (Wever et al., 2014). In ~~this~~ that study, a comparison of snowpack runoff measured by a snow lysimeter with modelled snowpack runoff showed a higher agreement when simulating liquid water flow with RE, especially on the sub-daily time scale. Additionally, the arrival of meltwater at the base of the snowpack in spring was found to be better predicted. However, these results were solely based on an analysis of liquid water outflow. The study raised questions to what ~~extend~~ extent the two water transport schemes differ in the simulation of the internal snowpack structure and whether the improvements in snowpack runoff estimations with RE are also consistent with simulations of the internal snowpack.

For many applications, especially in hydrological studies, the primary variables of interest are snow water equivalent (SWE) and snowpack runoff, as the first provides possible future meltwater and the latter provides the liquid water that directly participates in hydrological processes. In spite of its importance, direct measurements of SWE are relatively sparse. In contrast, snow height measurements are relatively easy to obtain either manually or automatically, and long climatological records of snow height are available. Methods have been developed to relate snow height to SWE (Jonas et al., 2009; Sturm et al., 2010). Snow density is another parameter that is variable in time and space (Bormann et al., 2013) and rather cumbersome to measure in the field. Although it is seldom of primary interest, it may serve wide applications as an intermediate parameter between a property that is observed and a property that one is interested in. For example, proper estimates of snow density will

increase the accuracy of translating snow height to SWE. Snow density is also required for the conversion of measured two-way travel time (TWT) from radar applications to snow depth in dry-snow conditions (Gubler and Hiller, 1984; Lundberg and Thunehed, 2000; Marshall et al., 2007; Heilig et al., 2009, 2010; Okorn et al., 2014) or translating dielectric measurements to liquid water content, as for example with the Snow Fork (Sihvola and Tiuri, 1996), or the Denoth meter (Denoth, 1994).

Apart from bulk snowpack properties, there is also a demand for detailed snowpack models to assess the layering and microstructural properties of the snowpack, for example with the purpose of avalanche forecasting. Layer transitions within the snow cover with pronounced contrasts in for example density, grain shape or grain size can act as zones in which fractures can be initialized and slab avalanches release (Schweizer et al., 2003). The presence of liquid water can reduce the strength of a snowpack considerably (Colbeck, 1982; Conway and Raymond, 1993), ~~for which Techel et al. (2011) showed a grain shape dependence.~~ Techel et al. (2011) showed that this reduction of strength depends also on the grain shape in the snow layers. When snowpack models are used to understand wet snow avalanche formation, it is important that the model can reproduce capillary barriers, at which liquid water may pond (Schneebeli, 2004; Baggi and Schweizer, 2009; Hirashima et al., 2010; Mitterer et al., 2011b). Also the arrival of meltwater at the bottom of the snowpack is considered to be a good indicator for the onset of wet snow avalanche activity. However, reliable liquid water content (LWC) measurements for the snowpack are difficult to obtain. Some attempts for continuous monitoring are promising (Schmid et al., 2014; Koch et al., 2014; Avanzi et al., 2014), but are not yet operational. Recently, Mitterer et al. (2011a) and Schmid et al. (2014) demonstrated the potential of upward-looking ground-penetrating radar (upGPR) to monitor the progress of the meltwater front and Heilig et al. (2015) present data for quasi continuous observations of bulk liquid water content over several years and for three different test sites. Here, their results concerning the position of the meltwater front will be compared with snowpack simulations. We also consider temperature measurements taken during manual snow profiling as a reliable and precise way to determine which part of the snowpack ~~has become at~~ is at the melting point (often termed

isothermal) and likely contains a fraction of liquid water due to infiltration (i.e. the movement of liquid water in snow) or local snowmelt.

As with snow density, snow temperatures are rarely of primary interest in snow studies. However, a correct representation of the temperature profile of the snowpack is required, as it has a large influence on the snow metamorphism (grain shape and size) and settling rates (Lehning et al., 2002a). Temperature gradients drive moisture transport and have a strong influence on the grain growth (Colbeck, 1982; Pinzer et al., 2012; Domine et al., 2013). Furthermore, temperature profiles are an indicator of whether the combination of the surface energy balance, the ground heat flux, and the internal heat conductivity of the snowpack is ~~correctly~~ adequately approximated.

In this study, the SNOWPACK model is driven by measurements from an automated weather station at Weissfluhjoch (WFJ) near Davos, Switzerland. Simulations are extensively verified for several bulk properties of the snowpack and against snow profiles made at WFJ, with the aim to verify the representation of the internal snowpack structure. Time series of soil and snow temperatures, snow lysimeter measurements and upGPR data from WFJ are used to validate snowpack temperature profiles, snowpack runoff and the progress of the meltwater front within the snowpack in the simulations. This study focusses on snowpack variables that are influenced by liquid water flow with the aim of a more in-depth comparison of differences between RE and the conventional bucket scheme. The comparison is limited to snow height, SWE, liquid water runoff from the snow cover, snow density, snow temperature, and grain size and shape, as for these variables, validation data are available. Internally, the SNOWPACK model also uses additional state variables, like sphericity, dendricity and bond size (Lehning et al., 2002a).

2 Theory

The theoretical basis of the SNOWPACK model regarding the heat ~~advection~~ transport equation and snow settling has been discussed in Bartelt and Lehning (2002). The treatment of the snow microstructure and several parametrisations, as for example for snow

viscosity, snow metamorphism and thermal conductivity, are presented in Lehning et al. (2002a). Some of those parametrisations have been refined in later versions of SNOWPACK. The treatment of the meteorological forcing for determining the energy balance at the snow surface is discussed in Lehning et al. (2002b). Finally, the liquid water transport schemes are presented and verified in Wever et al. (2014). Here, we will outline theoretical aspects not discussed in the aforementioned literature.

2.1 Water retention curves

Richards equation (RE) in mixed form reads (Richards, 1931; Celia et al., 1990) :

$$\frac{\partial \theta}{\partial t} - \frac{\partial}{\partial z} \left(K(\theta) \left(\frac{\partial h}{\partial z} + \cos \gamma \right) \right) + s = 0, \quad (1)$$

where θ is the volumetric liquid water content (LWC, $\text{m}^3 \text{m}^{-3}$), K is the hydraulic conductivity (m s^{-1}), h is the pressure head (m), z is the vertical coordinate (m, positive upwards and perpendicular to the slope), γ is the slope angle and s is a source/sink term ($\text{m}^3 \text{m}^{-3} \text{s}^{-1}$).

To solve RE this equation, the water retention curve and the saturated hydraulic conductivity K_{sat} (m s^{-1}) need to be specified. For the water retention curve, the van Genuchten model is used (van Genuchten, 1980). ~~It uses:~~

$$\theta = \theta_r + (\theta_s - \theta_r) \frac{(1 + (\alpha|h|)^n)^{-m}}{S_c}. \quad (2)$$

The water retention curve is then described by several parameters: residual water content θ_r ($\text{m}^3 \text{m}^{-3}$), saturated water content θ_s ($\text{m}^3 \text{m}^{-3}$) and parameters α (m^{-1}), n (–) and m (–). We correct the water retention curve using the approach by Ippisch et al. (2006) for taking into account the air entry pressure. As in Wever et al. (2014), an air entry pressure of 0.0058 m was used, corresponding to a largest pore size of 5 mm. Note that the residual

water content in the water retention curve, which is the dry limit, is not comparable to the water holding capacity or irreducible water content in the bucket scheme, which refers to wet conditions. For the soil part, the ROSETTA class average parameters (Schaap et al., 2001) are implemented to provide these parameters for various soil types.

For snow, the parametrisation for α in the van Genuchten model as proposed by Yamaguchi et al. (2010) reads:

$$\alpha = 7.3(22000r_g) + 1.9, \quad (3)$$

where $2r_g$ is the classical grain size (m), which is defined as the average maximum extent of the snow grains (Fierz et al., 2009). For n , the original parametrisation by Yamaguchi et al. (2010) was modified by Hirashima et al. (2010) to be able to extend the parametrisation beyond grain radii of 2 mm:

$$n = 15.68e^{\frac{(-0.46(2r_g))(-0.46(2000r_g))}{2000r_g}} + 1. \quad (4)$$

Here, we will abbreviate this parametrisation of the water retention curve as Y2010. This parametrisation has been used in Wever et al. (2014).

The Y2010 parametrisation was determined for snow samples with similar densities. In Yamaguchi et al. (2012), an updated set of experiments was described for a wider range of snow density and grain size, leading to the following parametrisation of the van Genuchten parameters:

$$\alpha = 4.4 \cdot 10^6 \left(\frac{\rho}{2r_g} \right)^{-0.98}, \quad (5)$$

and

$$n = 1 + 2.7 \cdot 10^{-3} \left(\frac{\rho}{2r_g} \right)^{0.61}, \quad (6)$$

where ρ is the dry density of the snowpack (kg m^{-3}). This parametrisation will be referred to as Y2012. Both parametrisations will be compared here. θ_r and θ_s are defined as described

in Wever et al. (2014) and K_{sat} is parametrised following Calonne et al. (2012)¹:

$$K_{\text{sat}} = \left(\frac{\rho_w g}{\mu} \right) \left[\frac{0.75}{1000} \frac{r_{\text{es}}}{3.0 r_{\text{es}}}^2 \exp(-0.013 \theta_i \rho_{\text{ice}}) \right], \quad (7)$$

where ρ_w and ρ_{ice} are the density of water (1000 kg m⁻³) and ice (917 kg m⁻³), respectively, g is the gravitational acceleration (taken as 9.8 m s⁻²), μ is the dynamic viscosity (taken as 0.001792 kg (m s)⁻¹), θ_i is the volumetric ice content (m³ m⁻³) and r_{es} is the equivalent sphere radius (m), approximated by the optical radius, which in turn can be parametrised using grain size, sphericity and dendricity (Vionnet et al., 2012).

In both parametrisations and for soil layers, the van Genuchten parameter m is chosen as:

$$m = 1 - (1/n), \quad (8)$$

such that the Mualem-model for the hydraulic conductivity in unsaturated conditions has an analytical solution (van Genuchten, 1980). ~~We correct the water retention curve using the approach by Ippisch et al. (2006) for taking into account the air entry pressure. As in Wever et al. (2014), an air entry pressure of 0.0058m was used, corresponding to a largest pore size of 5mm.~~

The method to solve RE requires the calculation of the hydraulic conductivity at the interface nodes. It is common to take the arithmetic mean (denoted AM) of the hydraulic conductivity of the adjacent elements, although other calculation methods have been proposed (e.g., see Szymkiewicz and Helmig, 2011). Here, we compare the default choice of AM with the geometric mean (denoted GM), as proposed by Haverkamp and Vauclin (1979), to investigate the possible influence of the choice on averaging method on the simulations of liquid water flow.

¹In Wever et al. (2014), this equation is also listed and contains an error: in that study, the factor 0.75 is used, which would correspond to r_{es} being the grain size, whereas 3.0 corresponds to the actually used definition of r_{es} being the grain radius.

2.2 Soil freezing and thawing

Due to the isolating effects of thick snow covers and the generally upward directed soil heat flux, soil freezing at WFJ is mostly limited to autumn and the beginning of the winter, when the snow cover is still shallow. To solve phase changes in soil, we follow the approach proposed by Dall'Amico et al. (2011). They express the freezing point depression in soil as a function of pressure head as:

$$T^* = T_{\text{melt}} + \frac{gT_{\text{melt}}}{L}h, \quad (9)$$

where T^* is the melting point of the soil water (K), T_{melt} is the melting temperature of water (273.15 K), L is the latent heat associated with the phase transition from ice to water (334 kJ kg⁻¹) and h is the pressure head (m).

When the soil temperature T (K) is at or below T^* , the soil is in freezing or thawing state and a mixture of ice and liquid water is present. Then, the pressure head associated with liquid water h_w (the liquid water part (h_w , m)) can be expressed as:

$$h_w = h + \frac{L}{gT^*}(T - T^*), \quad (10)$$

where h is the total pressure head of the soil (m). The van Genuchten model provides the relationship between pressure head and LWC:

$$\theta = \theta_r + (\theta_s - \theta_r) \frac{(1 + (\alpha|h_w|)^n)^{-m}}{\text{Sc}}, \quad (11)$$

where θ is the volumetric LWC (m³ m⁻³). Consequently, the ice part can be expressed as:

$$\theta_i = \theta_r + (\theta_s - \theta_r) \frac{(1 + (\alpha|h|)^n)^{-m}}{\text{Sc}} - \theta, \quad (12)$$

where Sc is the correction proposed by Ippisch et al. (2006).

In Dall'Amico et al. (2011), a splitting method is introduced to solve both the heat **advection-transport** equation and RE for liquid water flow in a semi-coupled manner. We approach the problem by finding the steady state solution for T , θ and θ_i in Eqs. (10), (11) and (12). This steady state solution is found numerically by using the Bisection–Secant method (Dekker, 1969), where the starting points for the method are taken as all ice melting and all liquid water freezing, respectively. In soil, liquid water flow can advect heat when a temperature gradient is present. In the soil module of SNOWPACK, heat advection associated with the liquid water flow is calculated after every time step of the RE solver, before assessing soil freezing and thawing.

3 Data and methods

3.1 Data (1): meteorological time series

The SNOWPACK model is forced with a meteorological data set from the experimental site Weissfluhjoch (WFJ) at an altitude of 2540m in the Swiss Alps near Davos ([Wever et al., 2015](#)). This measurement site is located in an almost flat part of a southeasterly oriented slope. During the winter months, a continuous seasonal snow cover builds up at this altitude. The snow season is defined here as the main consecutive period with a snow cover of at least 5 cm on the ground during the winter months, and is denoted by the year in which they end. The snow season at WFJ generally starts in October or November and lasts until June or July.

The data set contains air temperature, relative humidity, wind speed and direction, incoming and outgoing longwave and shortwave radiation, surface temperature, soil temperature at the interface between the snowpack and the soil, snow height, and precipitation from a heated rain gauge (Marty and Meister, 2012; Schmucki et al., 2014). An undercatch correction is applied for the measured precipitation (Wever et al., 2014). Snow temperatures are measured at 50, 100 and 150 cm above the ground surface, using vertical rods placed approximately 30 cm apart. From September 2013 onwards, soil temperatures are

measured at 50, 30 and 10 cm depth. The experimental site is also equipped with a snow lysimeter with a surface area of 5 m², as described in Wever et al. (2014). The rain gauge and snow lysimeter ~~are measuring~~ measure at an interval of 10 min, whereas most other measurements are done at 30 min intervals.

In the area surrounding WFJ, field data to validate soil freezing and thawing are lacking. For modelling the snowpack, the most important influence of the soil is the heat flux that is provided at the lower boundary of the snowpack. For this purpose, we will use the temperature measured at the interface between the soil and the snowpack to validate the soil module. This temperature measurement is influenced by soil freezing and thawing. Our primary interest here is the investigation to what degree the previously described soil module of SNOWPACK is capable of providing a realistic lower boundary for the snowpack in the simulations.

SNOWPACK can be forced with either measured precipitation amounts or with measured snow height. In precipitation-driven simulations (Precip driven), measured precipitation is assumed to be snowfall when the air temperature is below 1.2 °C and rain otherwise. For these type of simulations, the study period is from 1 October 1996 to 1 July 2014 (1 week after melt out date), consisting of 18 full snow seasons. In case of snow height-driven simulations (HS driven), an additional threshold for relative humidity (≥ 70%) and a maximum value for the temperature difference between the ~~snow surface and the air~~ air and the snow surface (≤ 3 °C) is used to determine whether snowfall is possible. The latter condition tests for cloudy conditions, when the increase in incoming longwave radiation will warm the snowpack surface close to air temperature. Then, snowfall is assumed to occur when measured snow height ~~is exceeding~~ exceeds the modelled snow height (Lehning et al., 1999) ~~; in combination with a parametrisation for~~ and consequently, new snow layers are added to the model domain in order to match the measured snow height again. These layers are initialized with a new snow density dependent on meteorological conditions (Schmucki et al., 2014). In both modes, new snow layers are added for each 2 cm of new snow. An uninterrupted, consistent dataset for this type of simulations is available from 1 October 1999 to 1 July 2014, consisting of 15 full snow seasons. The last snow season (2014) of the

studied period has the most data available and will be used as the example snow season to explain how SNOWPACK simulates the snow cover. Results for the other snow seasons are included in the online Supplement.

Many processes in SNOWPACK are based on physical descriptions that require calibration, for example for wet and dry snow settling, thermal conductivity and new snow density. For this purpose, dedicated datasets with some additional detailed snowpack measurements from snow seasons 1993, 1996, 1999 and 2006 have been used when constructing the model. Snow metamorphism processes were mainly calibrated against laboratory experiments (Bauach et al., 2001).

3.2 Data (2): manual snow profiles

Every two weeks, around the 1st and 15th of each month respectively (depending on weather conditions), a manual full depth snow profile is taken at ~~the WFJ~~ [WFJ \(Wever, 2015\)](#), following the guidelines from Fierz et al. (2009). [The snow profiling is carried out in the morning hours, starting around 09:00 LT.](#) Measurements include snow temperature at a resolution of 10 cm, and snow density in steps of approximately 30 cm. ~~Density is~~ [Snow density and SWE are](#) determined by taking snow cores using a 60 cm high aluminium cylinder with a cross-sectional area of 70 cm² ~~and weighting the snow core inserted vertically into the snowpack. The snow core is then weighted~~ using a calibrated spring. ~~SWE is determined from these density measurements.~~ For comparison with the simulations, SWE values are corrected for differences in snow height at the snow pit and at the automatic weather station, to eliminate the effect of spatial variability. Grain size (following the classical definition of average maximum extent of the snow grains) and grain shape are evaluated by the observer using a magnifying glass. ~~The snow profiling is carried out in the morning hours, starting around 09:00~~ [Also snow wetness is reported in five wetness classes as well as hand hardness in six classes \(Fierz et al., 2009\).](#) ~~Because judging snow wetness has a subjective component and estimating the actual LWC is generally considered rather difficult, we consider here only three categories: dry (class 1, 0% LWC), moist (class 2, 0-3% LWC) and wet (class 3 or higher, > 3% LWC).~~

3.3 Data (3): upward-looking ground-penetrating radar

An upGPR is located within the test site at a distance of approximately 20 m from the meteorological station (Mitterer et al., 2011a; Schmid et al., 2014). The upGPR is buried in the ground with the top edge level to the ground surface and points skyward. The radar instrument and data processing is described in Schmid et al. (2014). Measurement intervals for all observed melt seasons were set to 30 min during daytime. The only difference in the processing scheme applied for this study in comparison to Schmid et al. (2014) is that for an optimized retrieval of the dry-wet transition within the snow cover, we reduced the length of the moving-window time filter to a few days (1–3) instead of six weeks. Since percolating water results in strong amplitude increases at the respective depth of percolation and a decrease in wave speed for electromagnetic waves travelling through wet layers, we searched for occurrences of sharp amplitude contrasts together with diurnal variations in the location of signal responses of the overlying layers. For snow layers in which liquid water is appearing during the day and refreezing during the night, or when LWC reduces through outflow, a clear diurnal cycle in two-way travel time (TWT) of the respective signal reflections can be observed. Schmid et al. (2014) describe first attempts to determine ~~percolations~~ percolation depths automatically within the recorded radargrams. For this study, we manually determined all observations of the dry-wet transition in the snowpack and converted TWT in height above the radar by assuming a constant wave speed in dry snow of 0.23 m ns^{-1} (Mitterer et al., 2011a; Schmid et al., 2014). Data on liquid water percolation measured with upGPR have been presented in Schmid et al. (2014) for the snow seasons 2011 and 2012. Here, we present data of two more snow seasons (2013, 2014) and compare all measured depths of the dry-wet transition with simulation results. In snow seasons 2011, 2013 and 2014, additional snow profiles were made in close proximity of the upGPR, with a higher frequency during the melt season than the regular snow profiles discussed in the previous section.

3.4 Methods (1): model setup

For the simulations in this study, the SNOWPACK model ~~is solving~~ solves the energy balance at the snow surface. The turbulent fluxes are calculated using the stability correction functions as in Stössel et al. (2010). This is an adequate approximation for most of the snow season, when the snow surface cooling due to net outgoing long wave radiation ~~is causing~~ causes a stable stratification of the atmospheric boundary layer. The surface albedo is calculated from the ratio of measured incoming and reflected shortwave radiation. The net longwave radiation budget is ~~also calculated~~ determined from the difference in measured incoming and calculated outgoing long wave radiation. The aerodynamic roughness length (z_0) of the snow is fixed to 0.002 m.

The soil at WFJ consists of coarse material with some loam content, as was observed when installing the soil temperature sensors. The ROSETTA class average parameters for the loamy sand class are taken for the van Genuchten parametrisation of the water retention curve for the soil ($\theta_r = 0.049 \text{ m}^3 \text{ m}^{-3}$, $\theta_s = 0.39 \text{ m}^3 \text{ m}^{-3}$, $\alpha = 3.475 \text{ m}^{-1}$, $n = 1.746$, $K_{\text{sat}} = 1.2176 \cdot 10^{-5} \text{ m s}^{-1}$). For the thermodynamic properties, the specific heat for the soil constituents was set to $1.0 \text{ kJ kg}^{-1} \text{ K}^{-1}$ and the heat conductivity to $0.9 \text{ W m}^{-1} \text{ K}^{-1}$. The total soil depth in the model is taken as 3 m, with a variable layer spacing of 1 cm in the top layers and 40 cm for the lowest layer. The dense layer spacing in the top of the soil is necessary to describe the large gradients in soil moisture and temperature occurring here. At the lower boundary, a water table is prescribed, together with a Neumann boundary condition for the heat ~~advection~~ transport equation, simulating a constant geothermal heat flow of 0.06 W m^{-2} .

All simulations are run on the same desktop computer as a single-core process, using a model time step of 15 min. In the solver for RE, the SNOWPACK time step may be subdivided in smaller time steps when slow convergence is encountered (Wever et al., 2014). The computation time is in the order of a few minutes per year, where RE takes about twice as much time as the bucket scheme (Wever et al., 2014). Checks of the overall mass and energy balance reveal that the mass balance for all simulations is satisfied well within

1 mm w.e. and the energy balance error is generally around 0.05 W m^{-2} (see Table 1). We consider these errors to be well acceptable for our purpose.

3.5 Methods (2): analysis

The analysis of the simulations is done per snow season, ignoring summer snowfalls. The snow season at the WFJ is characterized by an early phase at the end of autumn or beginning of winter, when the snow cover is still relatively shallow and occasionally melt or rain-on-snow events are occurring. End of November to mid March can be defined as the accumulation period, in which snowpack runoff is virtually absent and the snowpack temperature is below freezing. This implies that in this period, all precipitation is added to the snow cover as solid mass, either by rain refreezing inside the snowpack, or by snowfall. Small amounts of snowmelt occurring near the surface refreeze during night or, after infiltration, inside the snowpack. Therefore, the increase in SWE between the biweekly profiles can be used to verify the undercatch correction in case the SNOWPACK model is driven with measured precipitation from the heated rain gauge, or to verify the combined effect of parametrised new snow density and snow settling in case snow height is used to derive snow fall amounts. The final phase is the melting phase, starting in April in most snow seasons, when the snowpack is isothermal and wet and produces snowpack runoff.

The snow temperature sensors may be influenced by penetrating shortwave radiation in the snowpack. Therefore, snow temperature measurements are only analysed when the measured snow height is at least 20 cm above the height of the sensor. Comparing snow temperatures between snow seasons was done by first standardising the measurement time of the temperature series between 0 and 1, for the start and end of the snow season, respectively. Then the data were binned in steps of 0.01 and bin averages were calculated. These series were then used for calculating the average and SD of differences between snow seasons. The same procedure was followed for snow height.

To compare manual snow profiles with the model simulations, several processing steps are required (Lehning et al., 2001). The snow height at the snow pit is generally different from the simulated snow height. This is not only due to the model not depicting the snow-

pack development perfectly but also because the snow pit is made at some distance from the snow height sensor which is used to drive the simulations. Therefore, we scale the simulated profile to the observed profile by adjusting each layer thickness, without adjusting the density. This implies that mass may be added or removed from the modelled domain. Then, the model layers are aggregated to match the number and thickness of the layers in the observations. Model layers are assigned to observed layers based on the centre height of the model layer. The typical thickness of a model layer is around 2 cm, so possible round-off errors are expected to be small. For temperature, the matching with modelled layer temperatures is achieved by linear interpolation from the measured temperature profile to the centre point of the modelled layer.

The cold content of the snowpack is the amount of energy necessary to bring the snowpack to 0 °C, after which an additional energy surplus will result in net snowmelt. The total cold content Q_{cc} (J m^{-2}) of the snowpack is defined in discrete form as the sum of the cold content of each layer:

$$Q_{cc} = \sum_{i=1}^n \rho_i c_i \Delta z_i (T_i - T_{\text{melt}}), \quad (13)$$

where i is an index to a snow layer, n is the number of snow layers in the domain, ρ_i is the density of the layer (kg m^{-3}), c_i is the specific heat of the layer ($\text{J kg}^{-1} \text{K}^{-1}$), Δz_i is the layer thickness (m) and T_i is the temperature of the layer (K). The cold content is calculated for both the observed and modelled profiles, where the modelled profile is first aggregated onto the observed layer spacing with the procedure described above.

4 Results and discussion

4.1 Snow height and snow water equivalent

Figure 1 shows the snow height for several simulation setups. Per construction, the snow height-driven simulations provide a high degree of agreement between measured and mod-

elled snow height. The general tendency of the precipitation-driven simulations is to follow the measured snow height, although it can be clearly seen that some precipitation events are overestimated, whereas others are underestimated. These differences are caused by inaccuracies when measuring solid precipitation with a rain gauge (Goodison et al., 1998), imperfections in the undercatch correction, or the effect of aeolian wind transport causing either erosion or accumulation of snow at the measurement site. As ~~snow drift is mainly occurring drifting snow mainly occurs~~ close to the surface, the rain gauge is rather insensitive to these effects as its installation height is higher than the typical depth of a ~~drifting snow saltation~~ layer. On the other hand, at WFJ, ~~snow drift drifting snow~~ is expected to play a relatively small role.

As listed in Table 1, the RMSE of snow height for all simulated snow seasons is significantly larger for precipitation-driven simulations than for snow height-driven ones. ~~Furthermore, the difference between~~ As snow height driven simulations are forced to closely follow the measured snow height, it can compensate for deviations in measured and modelled snow height ~~tends to be negative, denoting an underestimation of snow height by the model. In due to over- or underestimated snow settling or snow melt, and occasional erosion or deposition of snow by wind. This is not possible with precipitation driven simulations, that solely take precipitation amounts to determine snow fall. This contrast is additionally illustrated in~~ the Supplement Figs. S1 and S2, where snow height for the various model setups is shown for each snow season. Typical year-to-year variability of inconsistencies in the precipitation-driven simulations are present, whereas the snow height-driven simulations follow the measured snow height more closely. Consequently, the snow height driven simulations exhibit a better agreement on the melt out date, typically within one day from the observed melt out date, than the precipitation driven ones (see Table 1).

In Fig. 2, the average snow height difference is shown for all simulated snow seasons, relative to the standardized date in the snow season. ~~It shows that the underestimation~~ Snow height driven simulations generally have almost no bias to measured snow height for most of the snow ~~height is occurring mainly near~~ season. A slight positive bias in mid winter for precipitation driven simulations is caused by a few overestimated snow fall events, for which

the bias persists throughout the snow season (see for example snow season 2011-2012 in Fig.2e). Contrastingly, in the end of the snow season, thus during (i.e., the melt season), an underestimation of the snow height occurs in precipitation driven simulations, which is also expressed by a negative overall snow height bias in Table 1. This does not necessarily imply that the melt rates are overestimated, as snow height is the combined result of snow accumulation, settling and melt.

SWE is generally a better indicator of snow accumulation and snowmelt than snow height. A comparison between observed SWE in manual profiles and modelled SWE (Fig. 3a) shows that the agreement between both is high. The linear fits to the data points show that on average, the prediction of SWE in the model is accurate, for both snow height and precipitation-driven simulations. The scatter is larger for precipitation-driven simulations and there seems to be an underestimation of low SWE values and an overestimation of high ones.

The modelled SWE is a result of several effects: (i) snowfall amounts, which rely on an accurate estimation of new snow density in case of snow height-driven simulations or an adequate undercatch correction in case of precipitation-driven simulations, (ii) snow settling, in case of snow height-driven simulations, (iii) snowmelt and (iv) liquid water flow in snow and subsequent snowpack runoff. To separate the effects of liquid water flow and snowpack runoff from the other effects, Fig. 3b shows the increase in SWE in biweekly profiles during the accumulation phase of the snow season at ~~the~~ WFJ, when only factors (i), (ii), and (iii) ~~are playing play~~ a role. The snow height-driven simulations ~~are on average providing on average provide~~ a high degree of agreement with the measured increase in SWE during the accumulation phase, with only a marginal difference between the bucket scheme and RE. Here, it needs to be mentioned that in snow height-driven simulations, the snow settling formulation is able to compensate for errors in the estimation of new snow density and vice versa. For example: when new snow is initialized with a too high density, and thus too much mass is added, the snow settling will be underestimated and consequently, the next snow fall amount is also underestimated. Because the snowfall amounts in precipitation-driven simulations are independent of the settling of the snow cover, the increases in SWE are

independent of the predicted settling. ~~The results show~~ From the linear least squared fit to the observed and simulated changes in SWE, it can be concluded that in the accumulation phase, the combined effect of new snow density and snow settling ~~is providing~~ provides a slightly underestimated SWE increase in snow height-driven simulations, whereas the opposite is found for precipitation-driven simulations. In the latter case, particularly a few overestimated large snowfall events can be identified to have influenced the fit.

Figure 4 shows the difference in SWE between model simulations and the snow profiles for all simulated snow seasons. The difference in snow height-driven simulations is rather small, compared to precipitation-driven simulations. All simulations show that in the melt phase, the model underestimates SWE. This points towards either an overestimation of melt rates, or a too early release of meltwater at the base of the snowpack, or a combination of both. The fact that the discrepancies for the precipitation-driven simulations are larger than for the snow height-driven ones, is related to the underestimation of snow height during the melt phase. In the snow height-driven mode, an overestimated decrease in snow height during snowmelt is compensated for by a continuous adding of fresh snow ~~in case if~~ the snowfall conditions are met.

4.2 Liquid water content and snowpack runoff

Figure 5a and b show the distribution of liquid water within the snowpack for the example snow season 2014 for the bucket scheme and RE, respectively. Here, liquid water is present during the beginning of the snow season and during the melt season, which is a typical pattern for WFJ. The simulations with RE show a quicker downward routing of meltwater from the surface, where the meltwater is produced, than the simulations with the bucket scheme. Furthermore, the latter provides a rather homogeneous LWC distribution throughout the snowpack, except for the lighter surface elements, where LWC is significantly higher. A diurnal cycle is not visible in the simulations, except for layers close to the surface. With RE, there is both a strong variation in the vertical direction as well as in time. Marked accumulations of liquid water can be seen at transitions between layers with different characteristics. These accumulations peak ~~to at~~ around 10% LWC and ~~are occurring~~ occur during the first

wetting of the snowpack and above capillary barriers inside the snowpack. ~~Natural snow covers show such high LWC as well~~ The apparent slow downward movement of liquid water accumulations during the melt season results from snowpack settling moving the specific layers with water accumulations closer to the ground.

The formation of water accumulations on capillary barriers was also observed in natural snow covers (e.g., Techel and Pielmeier, 2011), and this process is considered to contribute to wet snow avalanche formation (Schneebeli, 2004; Baggi and Schweizer, 2009). ~~This~~ The effect is particularly present during the first wetting, as later in the melt season, wet snow metamorphism reduces the contrast between microstructural properties, and this is at least qualitatively reproduced by the model. Furthermore, the increase in hydraulic conductivity when the snowpack below the capillary barrier gets wet, reduces its function as a barrier. RE also introduces a strong diurnal cycle in LWC in the simulations. The results for other snow seasons can be found in the Supplement Figs. S3–S5, and they illustrate that the differences occurring between both water transport schemes in the example snow season are ~~consistent~~ similar for the other snow seasons as well.

Direct comparison of these model results with measurements is difficult, as continuous, non-destructive observations of the vertical distribution of LWC are not available. However, snowpack runoff is strongly coupled to the LWC distribution. Snowpack runoff at the measurement site WFJ ~~is typically occurring~~ typically occurs in the melt season and in some snow seasons during autumn when early snow falls may be ~~alternately followed~~ alternated by short melt episodes or rain-on-snow events. This is illustrated by the cumulative runoff curves in the Supplement Figs. S6 and S7. Table 1 shows the ratio of modelled to measured snowpack runoff. Snowpack runoff from precipitation-driven simulations is on average 2% less than observed, whereas snow height-driven simulations show about 8–14% more runoff than is observed. From the snow height-driven simulations, simulations with RE again have higher runoff sums than the simulations with the bucket scheme. This behaviour is found in most simulated snow seasons, as shown by Fig. ~~S8 in the Supplement~~ 6. The overestimation of total runoff in snow height-driven simulations is caused by the previously described mechanism where the snow height-driven simulations add snow layers in spring

when the snow height decrease is overestimated. The approach is inadequate during the melt season, as these new snow layers have low densities compared to the rest of the snowpack and snow settling will quickly reduce the modelled snow height again below the measured one. As the wet snow settling is a little stronger when using RE, this effect is slightly larger for those simulations.

A common measure to quantify the agreement between measured and modelled snowpack runoff is the Nash-Sutcliffe model efficiency (NSE, Nash and Sutcliffe (1970)), which is shown in Table 1 and Figs. [S9 and S10](#) [S8 and S9](#) in the Supplement for completeness. Further discussion can be found in Wever et al. (2014). NSE coefficients increase for simulations with RE, especially on the 1 hour time scale, as well as the r^2 value. [The decrease of performance in terms of NSE coefficient, in particular for the bucket scheme, can be mainly attributed to poor timing of melt water release during the day. For example, the bucket scheme does not take percolation time into account, resulting in rather low NSE coefficients. The](#) NSE coefficients and r^2 values tend to be lower for precipitation-driven simulations than for snow height-driven ones, especially in the simulations with RE. This likely is a result of a more accurate prediction of percolation time of liquid water through the snowpack in snow height-driven simulations. This is also indicated by the difference in time lag correlation (see Table 1) between precipitation-driven simulations and snow height-driven ones. The best timing of snowpack runoff on the hourly time scale is achieved with snow height-driven simulations with RE.

[The NSE coefficients and \$r^2\$ values reported here were calculated over the snow-covered period from the simulations. However, this is an arbitrary choice, given the discrepancies in melt out date from simulations and measurements, particularly for precipitation driven simulations \(see Table 1\). When considering both possible definitions for snow-covered period \(either determined from simulations or from measurements\), differences in NSE coefficients up to 0.16 are found for individual years. This is particularly the case for precipitation driven simulations, where the prediction of melt out date is less accurate \(see Table 1\). However, for the average NSE coefficients, the differences are less than 0.02 for both precipitation and snow height driven simulations, as the year-to-year differences cancel](#)

out. The choice of calculation period has a larger influence on r^2 values, since the late melt season is associated with the highest snowpack runoff, and consequently has a large effect on the r^2 values. Nevertheless, the differences between simulation setups within either snow height driven simulations or precipitation driven ones are smaller than the differences between both simulation types. This implies that the same conclusions about simulation setups can be drawn, regardless of the choice of calculation period.

4.3 Soil temperatures

At WJF, soil temperatures are available at three depths, but only for the last snow season in this study (see Fig. 7a). The simulated soil temperatures are ~~satisfactory~~ satisfactorily simulated, although the soil never showed temperatures well below 0 °C. This indicates that no significant soil freezing occurred, limiting the usefulness of these data to validate the new soil module. However, it is primarily important for this study that the soil as modelled by SNOWPACK serves as an adequate lower boundary condition for the snowpack simulations. For this purpose, we examine the soil temperature in the topmost soil part at the snow–soil interface, which is available for the snow seasons 2000–2014 (see Fig. 7b). For most of the time when a snow cover is present, the interface temperature at the snow–soil interface is close to 0 °C, except in the beginning of the snow season when the snow cover is still shallow. This is common for deep alpine snowpacks due to the isolating effect of thick snow covers and the generally upward directed soil heat flux. Figure 7b shows that the simulations capture the variability in early season soil–snow interface temperature to a high degree in most years and that the soil module in SNOWPACK is providing an accurate lower boundary for the snow cover in simulations.

4.4 Snow temperatures

Figure 8a and b show the simulated temperature distribution within the snowpack for the example snow season 2014 for the bucket scheme and RE, respectively. The other snow seasons are shown in the Supplement Figs. ~~S11–S13~~ S10–S12. For each snow season,

the snowpack temperature at WFJ is below freezing for an extended period of time and for these periods, no noticeable differences are found between simulations with the bucket scheme or RE. As a result of the differences in liquid water flow depicted in Fig. 5a and b, the parts of the snowpack that are isothermal differ significantly. Table 1 shows that the r^2 value between the relative part of the snowpack that is isothermal, as determined from measurements in the observed snow profiles and from the simulated ones, increases from 0.74 to 0.87 when solving liquid water flow with RE.

The temperature distribution of the snowpack is strongly related to the combination of the net energy balance of the snowpack and snow density. The latter influences the snow temperature through the thermal inertia of dense snow layers and through the strong ~~dependence of density on~~ density dependence of thermal conductivity (e.g., Calonne et al., 2011). Errors in either the energy balance or snow density may result in errors in snow temperatures. The cold content of the snowpack may be considered a more robust method to verify the simulated energy balance of the snow cover. Table 1 shows that the RMSE in cold content in the snow height-driven simulations is larger for the bucket scheme than RE, with a RMSE of around 670 kJ m^{-2} , which is equivalent to 2 mm w.e. snowmelt. This shows that the estimation of cold content in the simulations is adequate when, for example, estimating the onset of snowmelt and refreezing capacity inside the snowpack. Larger RMSE for precipitation-driven simulations can be associated with the larger discrepancy between measured and modelled snow height. The bias in the cold content is small compared to the RMSE, denoting that the average simulated energy input in the snowpack is accurate compared to its temporal variation. This conclusion is only valid for the period when the snowpack temperature is below freezing, as in the melt season, the cold content is by definition 0 J m^{-2} . ~~Furthermore, the surface energy balance is normally a self-balancing process, which is disrupted when phase changes occur.~~

Figure 9 a shows the measured and modelled snow temperature time series at three heights for the example snow season. The change of snow temperature over the snow season is adequately captured. There is almost no difference between simulations with the bucket scheme or RE, except for the timing when the snowpack gets isothermal, associated

with the meltwater front moving through the snowpack. For this example snow season, simulations with RE seem to better capture when the snowpack becomes 0 °C, suggesting a better prediction of the movement of the meltwater front through the snowpack. In the Supplement Figs. [S14 and S15](#)[S13 and S14](#), results for each snow season are shown. In most snow seasons, simulations with the RE provide a better agreement with measured temperatures in spring than the bucket scheme. However, in some snow seasons (e.g., 2001 and 2011), simulations with RE show an increase in snow temperature before the measured temperature increases, which ~~suggest a too fast~~ suggests a simulated progress of the meltwater front that is too fast.

In Fig. 10a and b, the average and SD, respectively, of the difference between modelled and measured temperatures are shown, including snow surface and snow–soil interface temperatures, determined over all 15 snow seasons of the snow height-driven simulations and plotted as a function of the relative date in the snow season. During the main winter season, the temperatures at 50 and 100 cm height are on average up to 0.5 °C lower in the model than in the measurements, whereas the temperature at 150 cm is on average up to 1.0 °C too high in the simulations. Interestingly the snow surface temperature is generally underestimated, whereas the temperature at the highest snow temperature sensor is too warmoverestimated in the simulations. The contrasting result suggests that the snow layers near the top of the snowpack have a too low density in the simulations. ~~This provides~~ , impacting both thermal conductivity and heat capacity of those layers, or the thermal conductivity is underestimated for typical snow densities found close to the surface. These effects provide a stronger isolation of the snowpack, causing heat from inside to escape at a slower rate and allowing the surface to cool more. ~~Errors~~ This offers an explanation why the underestimation of the snow surface temperature particularly occurs at night (not shown). In contrast, errors in diagnosing the snowpack energy balance ~~would be suspected~~ (i.e., in net shortwave or longwave radiation, or turbulent fluxes) would be expected to influence all temperature sensors in the same direction.

The SD of the difference between modelled and measured temperatures shows an increase with height above the ground. This can be attributed to higher temporal variations in

temperature in the upper snowpack due to highly variable surface energy fluxes. The SD for the snow and snow–soil interface temperature typically is less than 1.0 °C, and decreases towards the melt season. For the surface temperature, the SD is typically high in the beginning and the end of the snow season. In the beginning of the snow season, lower snow densities, low air temperatures and reduced incoming shortwave radiation allow for a strong radiative cooling of the snow surface, which is delicate to simulate correctly and may result in errors in simulated snow temperatures up to 10 °C. In the melt season, discrepancies in the duration the snow surface needs to refreeze at night may contribute to the increase in SD between modelled and measured surface temperatures.

Figure 10a also shows that in the beginning of the melt season, the difference between snow temperatures simulated with RE and measurements is on average smaller than with the bucket scheme at 0, 50 and 100 cm depth, ~~suggesting~~. Although this suggests a better timing of the movement of the meltwater front through the snowpack and the associated temperature increase to 0 °C, also heat advection through the ice matrix and preferential flow and subsequent refreezing inside the snowpack may increase the local snowpack temperature to 0 °C. The reason why ~~this is not expressed in the results from~~ the temperature series at 150 cm contrast those at 0, 50 and 100 cm depth remains unclear.

4.5 Snow density

Figure 11a and b show simulated snow density profiles for the bucket scheme and RE, respectively, for the example snow season 2014. In Supplement Figs. ~~S16–S18~~S15–S17, the other snow seasons are shown. Differences in density mainly arise when liquid water is involved. The accumulation and subsequent partial refreeze of meltwater at some layers form denser parts, whereas other layers remain less dense because less meltwater is retained. This type of stratification is known to happen, although verification is difficult, because density is sampled at a low spatial resolution in the manual snow profiles.

In Fig. 12a, average snow density as observed in the manual profiles is compared with the modelled snow densities for the snow height-driven simulations for the period 1999–2013. Generally, the seasonal trend in snow density is captured well in the model. Discrepancies

between modelled and observed profiles are larger than the differences arising from the different water transport schemes. In general, SNOWPACK overestimates the density near the base of the snow cover, while it underestimates the density of the upper part of the snowpack. This is consistent for all simulated snow seasons, as illustrated in Supplement Fig. S19S18. It supports the [argumentation-argument](#) in the previous section. These over- and underestimations are larger than the differences between water transport schemes. In Fig. 12b, the average and SD of the difference between simulated and observed density is shown, determined over the 15 snow seasons of the snow height-driven simulations. Average discrepancies in snow densities are less than 25 kg m^{-3} , increasing to $50\text{--}100 \text{ kg m}^{-3}$ shortly before melt out. The SD of the discrepancies is less than 50 kg m^{-3} , increasing to $100\text{--}150 \text{ kg m}^{-3}$ near the end of the melt season. This illustrates that the new snow density parametrisation and the snow settling formulation are able to provide accurate predictions of snow density. During the snow melt season, the deviations between observed and simulated snow density increase as a result of new snow fall events that are simulated to compensate for the overestimated SWE depletion.

The depletion rate is the result of many interacting processes. First of all, it is strongly coupled to snowmelt, and thus dependent on the surface energy fluxes. Given the high agreement in cold content in the main winter season, errors in diagnosing the surface energy balance due to uncertainties in atmospheric stability and measurement errors in radiation, wind speed or air temperature, seem to be small on average. However, a consistent or incidental overestimation of the energy input in the snow cover during the snow melt period may result in overestimated snow melt. Once the melt water is leaving the snowpack, the mass associated with it is definitely lost. Additionally, we would argue that an insufficient simulation of the densification during spring, under the influence of liquid water flow, may also be important here. A too low snow density will result in a deeper penetration of short-wave radiation, effectively providing heat transport into [the](#) snowpack. Furthermore, heat conductivity will be underestimated, with the consequence that the simulated snowpack in spring is too isolated to be able to release heat during night.

4.6 Grain size

Grain size plays an important role in liquid water flow, as it has a strong influence on the water retention curves (Eqs. 3–6). Figure 13a and b show modelled grain size profiles for the example snow season 2014 for the bucket scheme and RE, respectively. Differences between the schemes are mainly found in the melt season where the bucket scheme produces slightly larger grains. This is associated with the typically higher liquid water content using that scheme (Fig. 5a) compared to RE (Fig. 5b). This results in a stronger wet snow grain growth rate. Figure 13b also illustrates the cause of the liquid water accumulation found near a height of 120 cm in the beginning of April in Fig. 5b. The layer below the ponding water consisted of significantly larger grains and was creating a capillary barrier for the liquid water. In the Supplement Figs. [S20–S22](#)[S19–S21](#), results are shown for each snow season and a comparison with the LWC distribution (see Supplement Figs. S3–S5) shows that capillary barriers are a typical occurrence in simulations with RE for the deep, non-isothermal, stratified snow cover as found at WFJ. [For completeness, Figs. S23–S25 in the Supplement show simulated grain shapes for each snow season.](#)

Figure 14a and b show the average and SD of the grain sizes from the manual profiles and the simulations for the snow seasons 2000–2014. Most distinguishable is the steady increase in grain size towards and during the melt season. Both simulations show an increase in grain size towards the end of the snow season, although the average observed grain size is often underestimated. The underestimation of grain size in simulations with RE is consistent for most snow seasons compared to the bucket scheme. It results from generally lower LWC values in the snowpack in simulations with RE and, consequently, lower wet snow grain growth rates. This contributes to a reduced r^2 value for grain size (see Table 1). Most of the variation in grain size that exists before the initial wetting of the snow, remains present throughout the snow season in the simulations. However, the vertical variation of grain size typically decreases during the melt season, as shown in Fig. 14b. However, opposite trends can be found, mainly caused by snow falls during the melt season. The simulations tend to provide a decrease of the SD in the melt season and the agreement with the observa-

tions varies from year to year. Especially large variations in grain size in the profiles are not captured in the simulations.

4.7 Comparison of simulated dry-wet transition with upGPR

Detailed comparisons of radar-determined dry-wet transitions with simulations of the water transport schemes for the snow seasons 2011 through 2014 are presented in Fig. 15. Measured snowpack runoff (by the snow lysimeter) is included in this presentation together with grain shapes observed in snow pits, which both are indicative of water flow processes in snow. The dry-wet transition is only plotted when the upGPR signal indicated that parts of the snowpack were wet (see Sect. 3.3), or, for the simulations, when the modelled snowpack was partly wet. Due to beam divergence, a preferential flow path that forms in the vicinity above the upGPR could potentially be detected, although generally the upGPR would be particularly sensitive to matrix flow. However, liquid water accumulations above ponding layers are clearly visible in radargrams independent from matrix or preferential flow that formed such accumulations. It is impossible to discriminate from the radar data which flow regime caused the respective liquid water accumulations. In addition, layer transitions within the resolution limit of the radar (≈ 0.07 m for dry-snow conditions (Schmid et al., 2014)) are impossible to discriminate as well and as a consequence, percolation depths of the wetting front close to the ground surface (< 10 cm above the ground) cannot be accurately allocated anymore. Interferences with the reflection signal from the cover box of the radar prevent an accurate location of such signals.

From the four snow seasons presented in Fig. 15, the following observations can be made: (i) snowpack runoff measured by the snow lysimeter consistently starts earliest in the snow season. (ii) The progress of the meltwater front is always faster in the simulations with RE, compared to the bucket scheme. (iii) The radar-derived meltwater front progresses generally slower through the snowpack than in both water transport schemes in the model. (iv) The manual snow profiles mostly show melt forms in parts of the snowpack that have been wet according to the radar data, whereas the simulations often show larger parts of

the snowpack becoming wet earlier than indicated by the profiles. These observations will now be discussed in more detail.

(i) Since preferential flow can route liquid water efficiently through the snowpack (Kattelmann, 1985; Waldner et al., 2004; Techel and Pielmeier, 2011), upGPR-determined depths of dry-wet transitions are not necessarily linked to the onset of measured snowpack runoff (Heilig et al., 2015). Studies by Katsushima et al. (2013) and Hirashima et al. (2014) found that ponding plays a crucial role in forming preferential flow in both laboratory experiments as well as model simulations. The ponding of liquid water in the simulations for WFJ (see Fig. 5) suggests that preferential flow may have developed. The amount of snowpack runoff measured before the arrival of the meltwater front is highly variable. From 1 until 8 April in snow season 2011, large amounts of snowpack runoff were observed, most likely due to lateral flow processes, whereas in snow season 2014, only marginal amounts were observed. In the latter snow season, there is a strong increase in observed snowpack runoff close to the time of the arrival of the radar-derived meltwater front at the snowpack base. This variability between years is not necessarily caused by different preferential flow path structures, but may also result from the limited capturing area of the snow lysimeter (Kattelmann, 2000).

(iii, iv) The vertical distribution of the melt forms in the observed snow profiles may be considered particularly representative for matrix flow and for the four presented years it generally corresponds well with the parts of the snowpack that may be considered wet from the upGPR signal. (ii) As the bucket scheme shows a higher correspondence with the upGPR data than RE, the convenient improvement in the accuracy of simulated snowpack runoff with RE, as found in Wever et al. (2014), seems to be partly caused by (unintentionally) mimicking some preferential flow effects. To what extent this is caused by parametrisations of the water retention curve or hydraulic conductivity, or by the specifics of the implementation of RE in SNOWPACK, remains unclear. (ii, iii) Although the bucket scheme may seem to better coincide with the meltwater front in the upGPR data, it may as well be argued that the differences between both water transport schemes are smaller than the discrepancies with the upGPR data. It is likely that the limits of one-dimensional models with a single water

transport mechanism will prevent a correct simulation of both snowpack runoff as well as the internal snowpack structure at the same time.

In the beginning of the melt season, [when the meltwater front is disappearing regularly during night observations contrasting to the main melt phase discussed above can be made. The initial melt phase is characterized by a regularly disappearing meltwater front at night. During this period](#), the depth to which the liquid water infiltrates the snowpack is underestimated in the simulations. Here, the RE scheme shows larger infiltration depths, which are in better agreement with the upGPR data, although again differences between both simulations are smaller than the discrepancies with the upGPR data. This result is contradictory with the main melt phase, where the speed with which the meltwater front progresses through the snowpack is largely overestimated in the simulations. Furthermore, the distribution of melt forms in the snow profiles does not always coincide with the deeper infiltration depths detected by the upGPR.

An exception to the discussion above is snow season 2012, for which the results are consistent to a high degree. The progress of the meltwater front through the snowpack is accurately modelled by RE, and only slightly less accurately by the bucket scheme for this snow season when comparing with the upGPR signal. The snow lysimeter measurements show runoff almost directly at the time the meltwater front as detected from the upGPR reaches the soil. In the first snow profile made afterwards, melt forms were found for most parts of the snow cover. However, it is important to note that the progress of the meltwater front is much quicker than in the other snow seasons. Firstly, due to large snow falls in that snow season, the snow stratification was rather homogeneous, limiting the amount of possible capillary barriers or impermeable layers in the snowpack that could hinder the liquid water flow. The relatively homogeneous stratification can be found in snow density (Supplement Fig. [S18S17e,f](#)) as well as in grain size (Supplement Fig. [S22S21e,f](#)) and grain type (Supplement Fig. [S25e,f](#)). Second, the onset of the snowmelt was initiated by a very warm period, leading to sufficient snowmelt to infiltrate the complete snowpack in a short amount of time. These factors all provide fewer challenges for the model.

Figure 15 also illustrates the effects of the choice of averaging method for the hydraulic conductivity at the interface nodes. The progress of the meltwater front ~~is following~~ follows a stepwise pattern. The arithmetic mean ~~is reducing~~ reduces the contrast in hydraulic conductivity, causing a smearing of liquid water between layers as well as over microstructural transitions inside the snowpack. The geometric mean ~~is putting~~ puts more weight on the lowest hydraulic conductivity, which is found in dry snow. This results in a strengthened capillary barrier, indicated by the ~~temporal flatter~~ flatter temporal position of the meltwater front compared to the arithmetic mean.

4.8 Outlook

The extensive validation of the SNOWPACK model presented here has indicated several areas for future research and development. When focussing on processes directly impacted by liquid water flow, we can identify grain size and snow density as important properties, since they also influence hydraulic properties. It was found that during the spring melt season, both water transport schemes underestimated grain growth. Furthermore, indications were found that snow density in the melt season, which depends on the wet snow settling, is underestimated. This could be either a result of not fully representative parameterisations of these process in SNOWPACK, or an underestimation of LWC in the snowpack. The latter hypothesis is supported by the comparison of bulk LWC from simulations and upGPR measurements, which has revealed an underestimation of bulk LWC in both water transport schemes on the flat site WFJ (Heilig et al., 2015). Interestingly, this underestimation was not found on slopes, which leads to the proposed hypothesis that on a flat field, capillary barriers and ice lenses may introduce stronger ponding of liquid water inside the snowpack than on slopes, where water can flow laterally.

It was also identified here that SWE depletion rates in the SNOWPACK model for the measurement site WFJ are overestimated. The SWE depletion in spring is dependent on many factors, such as snow density and wet snow settling, influencing the heat capacity, internal heat fluxes and penetration of short wave radiation, as well as the surface energy balance and liquid water flow. These processes are difficult to investigate separately

and errors could also be introduced by errors in the meteorological measurements that are used to force the model. For verifying the surface energy balance, ideally, repeated cold content measurements could be performed using the calorimetric method. However, this type of measurement is rather cumbersome to perform in the field. Accurate turbulent flux measurements would allow to verify the parametrisations for latent and sensible heat. Snow compaction (settling) could be assessed with in-situ snow harps or snow profiles at a higher temporal resolution than only biweekly. In addition, recent advances in snow micro penetrometer (SMP) are also highly promising, allowing to achieve density measurements at high temporal and spatial resolution with relatively little effort (Schneebeli and Johnson, 1998; Proksch et al., 2015). A drawback of that method is that SMP measurements are not suitable for wet snow conditions.

The simulation of liquid water flow in snow currently only considers a one dimensional component, assuming homogeneity in the horizontal dimension. However, this is a very strong simplification. In reality, liquid water flow exhibits strong variation in three dimensions, due to preferential flow paths or flow fingering (Waldner et al., 2004; Techel and Pielmeier, 2011). The comparison of modelled liquid water flow with upGPR data and snowpack runoff measurements has identified that this simplification is indeed introducing representation errors. Numerical experiments (Hirashima et al., 2014) and laboratory observations (Katsushima et al., 2013) have provided promising indications that these processes could be described using Richards equation in three dimensions. At the same time, several processes that do appear in one dimensional simulations, as for example the ponding of liquid water on capillary barriers, seem to be essential in forming preferential flow paths. This possibly allows for a parameterization of preferential flow in the SNOWPACK model, that is closely linked to physical processes. Validation could be achieved by more detailed snow lysimeter studies, for example from measurement sites with multiple neighbouring lysimeters, improved laboratory experiments or further exploiting the upGPR data.

5 Conclusions

The one-dimensional physics based multi-layer SNOWPACK model has been evaluated against measured time series and manual snow profiles for the measurement site WFJ in the Swiss Alps near Davos. Two water transport schemes, the bucket scheme and RE, were taken into consideration as well as two modes to provide the precipitation forcing for the simulations: snow height-driven (15 snow seasons) and precipitation-driven (18 snow seasons). Along with the implementation of the solver for RE, the soil module of SNOWPACK has also been updated. Comparing simulated and measured temperatures at the snow–soil interface confirmed that the updated soil module can provide a correct lower boundary for the snowpack in the model.

The snow height-driven simulations provide good agreement with measured snow height (RMSE around 4 cm) and, during the accumulation phase of the snow cover, with SWE. This indicates that the model adequately simulates the combination of snow settling and new snow density. In precipitation-driven simulations, the SWE in the accumulation phase exhibits a slightly larger [spread error](#) than in snow height-driven simulations, which is mainly caused by deficiencies in the precipitation undercatch correction and possibly snow drift effects. This results in a lower RMSE for snow height (20–23 cm). For the simulations at WFJ, SNOWPACK consistently overestimates the depletion rate of SWE during the spring melt season, resulting in an underestimation of SWE of typically 200 mm w.e. near the end of the snow season, accompanied by an underestimation of snow height up to 30–40 cm. In snow height-driven simulations, this is compensated for by simulating regular snowfalls in order to match measured snow height. This procedure has as a drawback that too much mass is added to the snowpack in spring, resulting in an about 8–14 % overestimation of cumulative runoff over the snow season, whereas precipitation-driven simulations provide on average 2 % less snowpack runoff than measured.

The comparison of simulated snow density with snow density measurements made in snow profiles has shown that both the average snow density and the seasonal trend is well simulated in SNOWPACK during the main winter season. Average bias is around 25 kg m^{-3}

and the density of deep snow layers is slightly overestimated, whereas the density of upper layers is slightly underestimated. ~~The~~ In snow height-driven simulations, the discrepancies grow in the melt season, when SNOWPACK underestimates snow density on average by up to 100 kg m^{-3} as a result of new snow fall events that are simulated to compensate for over-estimated SWE depletion ~~in snow height-driven simulations~~. The model provides simulations of grain size which are consistent with observations in manual snow profiles. Although RE ~~is causing~~ causes a slight underestimation of grain size compared to the bucket scheme, snow density and grain size are adequately simulated for the parametrisation of the water retention curves.

Modelled and measured snow temperatures showed a satisfying agreement with average discrepancies of around $0.5 \text{ }^{\circ}\text{C}$. The discrepancies in the surface temperature were found to be larger, likely associated with the above mentioned underestimation of snow density in the upper layers and consequently the effect on thermal conductivity. The discrepancy in the cold content of the snow cover from simulations and field measurements was found to be small, suggesting that the surface energy balance and the soil heat flux are on average satisfactorily estimated. However, this conclusion only holds for the main winter period, as the defined cold content can only be used to assess energy budgets of snow that is below freezing.

The temporal evolution and the vertical distribution of the LWC in the snowpack differ significantly between the bucket scheme and RE. The latter provides a faster downward propagation of the meltwater front. This is accompanied by a higher r^2 value and NSE coefficient between simulated and measured snowpack runoff for the simulations with RE compared to the bucket scheme. RE also provides a higher r^2 value for the isothermal part of the snowpack compared to the manual snow profiles as well as a closer agreement with snow temperatures during the melt season. These results suggest a more accurate simulation of the progress of the meltwater front through the snowpack with RE. Although the data from the upGPR supports the deeper meltwater infiltration in the snowpack in the early melt phase as simulated with RE, the opposite is found for the main wetting phase. Additionally, the distribution of melt forms in the observed snow profiles shows a higher agreement with

the upGPR signal than with the simulations. Both type of observations may be considered particularly representative of matrix flow processes. The high agreement between simulations with RE and snowpack runoff therefore suggests that the use or implementation of RE is unintentionally mimicking preferential flow effects. However, the differences between both water transport schemes are relatively small, compared to the differences between simulations and the observed melt water front in the upGPR data. The results suggest that the ability of a one-dimensional approach to correctly estimate both snowpack runoff as well as the internal snowpack structure in wet snow conditions is rather limited. As the simulation of ponding of liquid water on capillary barriers and crusts is only captured with RE and not with the bucket scheme, RE seems promising however for the ability of SNOWPACK to assess wet snow avalanche risks. Future studies may also focus on the possibilities to assimilate radar derived vertical snowpack structure (e.g., density, ice layers, liquid water) into the SNOWPACK model. This would allow to better understand to what ~~extend~~extent discrepancies between simulations and radar data ~~is~~are caused by deviations in the simulated snowpack state at the onset of snowmelt or by an insufficient process representation in the model.

The validation has shown that SNOWPACK has sufficient agreement with measurements for snow temperatures, snow density and grain size in the main winter season for a wide range of applications. When using RE, we found that the Y2012 water retention curve provides better results than the Y2010 parametrisation, whereas different averaging methods to determine the hydraulic conductivity at the nodes between layers seem to have little influence. In general, several aspects of the simulations related to liquid water flow improve with RE, although often, the differences between simulations tend to be smaller than differences between the simulations and the observations and the improvements are often inconsistent with the representation of the internal snowpack structure as indicated by the upGPR data.

**The Supplement related to this article is available online at
doi:10.5194/tcd-0-1-2015-supplement.**

Acknowledgements. ~~This research~~ The meteorological forcing data from WFJ, including snow lysimeter data, is published as Wever et al. (2015) and the data from the biweekly snow profiles as Wever (2015). We thank the Swiss Federal Office of Meteorology and Climatology (MeteoSwiss) for providing quality controlled precipitation data from Weissfluhjoch, which can be obtained via IDAWEB (<https://gate.meteoswiss.ch/idaweb>). The SNOWPACK source code is available under the GNU Lesser General Public Licence Version 3 and can be accessed at: <http://models.slf.ch>. The exact version of the SNOWPACK model used in this study corresponds to SVN revision number 652 of the version available in /branches/dev/, including a patch (available at the repository) of a few changes that were incorporated in later updates to the model. Data from the upGPR is available at the authors upon request. The research presented here has been conducted in the framework of the IRKIS project supported by the Office for Forests and Natural Hazards of the Swiss Canton of Grisons (C. Wilhelm), the region of South Tyrol (Italy) and the community of Davos. L. Schmid has been supported within the framework of the D-A-CH consortium (DFG-FWF-SNF) with the German Research Foundation (DFG) as lead agency. A. Heilig was supported by DFG grant EI 672/6; and O. Eisen by the DFG Emmy Noether programme grant EI 672/5. We also thank ~~are~~ thankful to the many employees of the institute involved in taking the biweekly snowpack profiles at ~~the~~ Weissfluhjoch for many years.

References

- Avanzi, F., Caruso, M., Jommi, C., Michele, C. D., and Ghezzi, A.: Continuous-time monitoring of liquid water content in snowpacks using capacitance probes: a preliminary feasibility study, *Adv. Water Resour.*, 68, 32–41, doi:10.1016/j.advwatres.2014.02.012, 2014.
- Baggi, S. and Schweizer, J.: Characteristics of wet-snow avalanche activity: 20 years of observations from a high alpine valley (Dischma, Switzerland), *Nat. Hazards*, 50, 97–108, doi:10.1007/s11069-008-9322-7, 2009.
- Bartelt, P. and Lehning, M.: A physical SNOWPACK model for the Swiss avalanche warning, Part I: numerical model, *Cold Reg. Sci. Technol.*, 35, 123–145, doi:10.1016/S0165-232X(02)00074-5, 2002.
- Baunach, T., Fierz, C., Satyawali, P. K., and Schneebeli, M.: A model for kinetic grain growth, *Ann. Glaciol.*, 32, 1–6, doi:10.3189/172756401781819427, 2001.

- Bormann, K. J., Westra, S., Evans, J. P., and McCabe, M. F.: Spatial and temporal variability in seasonal snow density, *J. Hydrol.*, 484, 63–73, doi:10.1016/j.jhydrol.2013.01.032, 2013.
- [Brun, E., Martin, E., Simon, V., Gendre, C., and Coléou, C.: An energy and mass model of snow cover suitable for operational avalanche forecasting, *J. Glaciol.*, 35, 333–342, 1989.](#)
- Calonne, N., Flin, F., Morin, S., Lesaffre, B., du Roscoat, S. R., and Geindreau, C.: Numerical and experimental investigations of the effective thermal conductivity of snow, *Geophys. Res. Lett.*, 38, L23501, doi:10.1029/2011GL049234, 2011.
- Calonne, N., Geindreau, C., Flin, F., Morin, S., Lesaffre, B., Rolland du Roscoat, S., and Charrier, P.: 3-D image-based numerical computations of snow permeability: links to specific surface area, density, and microstructural anisotropy, *Cryosphere*, 6, 939–951, doi:10.5194/tc-6-939-2012, 2012.
- [Celia, M. A., Bouloutas, E. T., and Zarba, R. L.: A general mass-conservative numerical solution for the unsaturated flow equation, *Water Resour. Res.*, 26, 1483–1496, doi:10.1029/WR026i007p01483, 1990.](#)
- Colbeck, S. C.: An overview of seasonal snow metamorphism, *Rev. Geophys.*, 20, 45–61, doi:10.1029/RG020i001p00045, 1982.
- Conway, H. and Raymond, C. F.: Snow stability during rain, *J. Glaciol.*, 39, 635–642, 1993.
- Dall’Amico, M., Endrizzi, S., Gruber, S., and Rigon, R.: A robust and energy-conserving model of freezing variably-saturated soil, *Cryosphere*, 5, 469–484, doi:10.5194/tc-5-469-2011, 2011.
- Dekker, T. J.: Finding a zero by means of successive linear interpolation, in: *Constructive Aspects of the Fundamental Theorem of Algebra*, edited by: Dejon, B. and Henrici, P., Wiley-Interscience, New York, 37–48, 1969.
- Denoth, A.: An electronic device for long-term snow wetness recording, *Ann. Glaciol.*, 19, 104–106, 1994.
- Domine, F., Morin, S., Brun, E., Lafaysse, M., and Carmagnola, C. M.: Seasonal evolution of snow permeability under equi-temperature and temperature-gradient conditions, *Cryosphere*, 7, 1915–1929, doi:10.5194/tc-7-1915-2013, 2013.
- Fierz, C., Armstrong, R., Durand, Y., Etchevers, P., Greene, E., McClung, D., Nishimura, K., Satyawali, P., and Sokratov, S.: *The International Classification for Seasonal Snow on the Ground (ICSSG)*, Tech. rep., IHP-VII Technical Documents in Hydrology No. 83, IACS Contribution No. 1, UNESCO-IHP, Paris, 2009.
- Goodison, B., Louie, P., and Yang, D.: *WMO Solid precipitation measurement intercomparison, Final Report*, Tech. rep., World Meteorological Organization (WMO), Geneva, 1998.

- Gubler, H. and Hiller, M.: The use of microwave FMCW radar in snow and avalanche research, *Cold Reg. Sci. Technol.*, 9, 109–119, doi:10.1016/0165-232X(84)90003-X, 1984.
- Haverkamp, R. and Vauclin, M.: A note on estimating finite difference interblock hydraulic conductivity values for transient unsaturated flow problems, *Water Resour. Res.*, 15, 181–187, doi:10.1029/WR015i001p00181, 1979.
- Heilig, A., Schneebeli, M., and Eisen, O.: Upward-looking ground-penetrating radar for monitoring snowpack stratigraphy, *Cold Reg. Sci. Technol.*, 59, 152–162, doi:10.1016/j.coldregions.2009.07.008, 2009.
- Heilig, A., Eisen, O., and Schneebeli, M.: Temporal observations of a seasonal snowpack using upward-looking GPR, *Hydrol. Proc.*, 24, 3133–3145, doi:10.1002/hyp.7749, 2010.
- Heilig, A., Mitterer, C., Schmid, L., Wever, N., Schweizer, J., Marshall, H.-P., and Eisen, O.: Seasonal and diurnal cycles of liquid water in snow ~~and effects on runoff, to be submitted to~~ Measurements and modeling, *J. Geophys. Res.*, doi:10.1002/2015JF003593, accepted, 2015.
- Hirashima, H., Yamaguchi, S., Sato, A., and Lehning, M.: Numerical modeling of liquid water movement through layered snow based on new measurements of the water retention curve, *Cold Reg. Sci. Technol.*, 64, 94–103, doi:10.1016/j.coldregions.2010.09.003, 2010.
- Hirashima, H., Yamaguchi, S., and Katsushima, T.: A multi-dimensional water transport model to reproduce preferential flow in the snowpack, *Cold Reg. Sci. Technol.*, 108, 80–90, doi:10.1016/j.coldregions.2014.09.004, 2014.
- Ippisch, O., Vogel, H.-J., and Bastian, P.: Validity limits for the van Genuchten–Mualem model and implications for parameter estimation and numerical simulation, *Adv. Water Resour.*, 29, 1780–1789, doi:10.1016/j.advwatres.2005.12.011, 2006.
- Jonas, T., Marty, C., and Magnusson, J.: Estimating the snow water equivalent from snow depth measurements in the Swiss Alps, *J. Hydrol.*, 378, 161–167, doi:10.1016/j.jhydrol.2009.09.021, 2009.
- Jordan, R.: A one-dimensional temperature model for a snow cover: Technical documentation SNTHERM.89, Tech. Rep. Spec. Rep. 657, U.S. Army Cold Reg. Res. Eng. Lab., Hanover, NH, 1991.
- Katsushima, T., Yamaguchi, S., Kumakura, T., and Sato, A.: Experimental analysis of preferential flow in dry snowpack, *Cold Reg. Sci. Technol.*, 85, 206–216, doi:10.1016/j.coldregions.2012.09.012, 2013.
- Kattelman, R.: Macropores in snowpacks of Sierra Nevada, *Ann. Glaciol.*, 6, 272–273, 1985.

- Kattelmann, R.: Snowmelt lysimeters in the evaluation of snowmelt models, *Ann. Glaciol.*, 31, 406–410, doi:10.3189/172756400781820048, 2000.
- Koch, F., Prasch, M., Schmid, L., Schweizer, J., and Mauser, W.: Measuring snow liquid water content with low-cost GPS receivers, *Sensors*, 14, 20975–20999, doi:10.3390/s141120975, 2014.
- Lehning, M., Bartelt, P., Brown, B., Russi, T., Stöckli, U., and Zimmerli, M.: SNOWPACK calculations for avalanche warning based upon a new network of weather and snow stations, *Cold Reg. Sci. Technol.*, 30, 145–157, doi:10.1016/S0165-232X(99)00022-1, 1999.
TS8:
- Lehning, M., Fierz, C., and Lundy, C.: An objective snow profile comparison method and its application to SNOWPACK, *Cold Reg. Sci. Technol.*, 33, 253–261, doi:10.1016/S0165-232X(01)00044-1, 2001.
- Lehning, M., Bartelt, P., Brown, B., Fierz, C., and Satyawali, P.: A physical SNOWPACK model for the Swiss avalanche warning Part II: Snow microstructure, *Cold Reg. Sci. Technol.*, 35, 147–167, doi:10.1016/S0165-232X(02)00073-3, 2002a.
- Lehning, M., Bartelt, P., Brown, B., and Fierz, C.: A physical SNOWPACK model for the Swiss avalanche warning Part III: Meteorological forcing, thin layer formation and evaluation, *Cold Reg. Sci. Technol.*, 35, 169–184, doi:10.1016/S0165-232X(02)00072-1, 2002b.
- Lundberg, A. and Thunehed, H.: Snow wetness influence on impulse radar snow surveys theoretical and laboratory study, *Nord. Hydrol.*, 31, 89–106, 2000.
- Marshall, H.-P., Schneebeli, M., and Koh, G.: Snow stratigraphy measurements with high-frequency FMCW radar: comparison with snow micro-penetrometer, *Cold Reg. Sci. Technol.*, 47, 108–117, doi:10.1016/j.coldregions.2006.08.008, 2007.
- Marty, C. and Meister, R.: Long-term snow and weather observations at Weissfluhjoch and its relation to other high-altitude observatories in the Alps, *Theor. Appl. Climatol.*, 110, 573–583, doi:10.1007/s00704-012-0584-3, 2012.
- Mitterer, C., Heilig, A., Schweizer, J., and Eisen, O.: Upward-looking ground-penetrating radar for measuring wet-snow properties, *Cold Reg. Sci. Technol.*, 69, 129–138, doi:10.1016/j.coldregions.2011.06.003, 2011a.
- Mitterer, C., Hirashima, H., and Schweizer, J.: Wet-snow instabilities: comparison of measured and modelled liquid water content and snow stratigraphy, *Ann. Glaciol.*, 52, 201–208, doi:10.3189/172756411797252077, 2011b.
- Nash, J. and Sutcliffe, J.: River flow forecasting through conceptual models, part I – a discussion of principles, *J. Hydrol.*, 10, 282–290, doi:10.1016/0022-1694(70)90255-6, 1970.

- Okorn, R., Brunnhofer, G., Platzer, T., Heilig, A., Schmid, L., Mitterer, C., Schweizer, J., and Eisen, O.: Upward-looking L-band FMCW radar for snow cover monitoring, *Cold Reg. Sci. Technol.*, 103, 31–40, doi:10.1016/j.coldregions.2014.03.006, 2014.
- Pinzer, B. R., Schneebeli, M., and Kaempfer, T. U.: Vapor flux and recrystallization during dry snow metamorphism under a steady temperature gradient as observed by time-lapse microtomography, *Cryosphere*, 6, 1141–1155, doi:10.5194/tc-6-1141-2012, 2012.
- [Proksch, M., Rutter, N., Fierz, C. and Schneebeli, M.: Intercomparison of snow density measurements: bias, precision and spatial resolution, *Cryosphere Discuss.*, 9, 3581–3616, doi:10.5194/tcd-9-3581-2015, 2015.](#)
- [Richards, L.: Capillary conduction of liquids through porous mediums, *J. Appl. Phys.*, 1, 318–333, doi:10.1063/1.1745010, 1931.](#)
- Schaap, M. G., Leij, F. J., and van Genuchten, M. T.: ROSETTA: a computer program for estimating soil hydraulic parameters with hierarchical pedotransfer functions, *J. Hydrol.*, 251, 163–176, doi:10.1016/S0022-1694(01)00466-8, 2001.
- Schmid, L., Heilig, A., Mitterer, C., Schweizer, J., Maurer, H., Okorn, R., and Eisen, O.: Continuous snowpack monitoring using upward-looking ground-penetrating radar technology, *J. Glaciol.*, 60, 509–525, doi:10.3189/2014JoG13J084, 2014.
- Schmucki, E., Marty, C., Fierz, C., and Lehning, M.: Evaluation of modelled snow depth and snow water equivalent at three contrasting sites in Switzerland using SNOWPACK simulations driven by different meteorological data input, *Cold Reg. Sci. Technol.*, 99, 27–37, doi:10.1016/j.coldregions.2013.12.004, 2014.
- Schneebeli, M.: Mechanisms in wet snow avalanche release, in: Proceedings ISSMA-2004, International symposium on snow monitoring and avalanches. Snow and Avalanche Study Establishment, India, Manali, India, 12–16 April 2004, pp. 75–77, 2004.
- [Schneebeli, M. and Johnson, J.: A constant-speed penetrometer for high-resolution snow stratigraphy, *Ann. Glaciol.*, 26, 107–111, 1998.](#)
- Schweizer, J., Jamieson, J. B., and Schneebeli, M.: Snow avalanche formation, *Rev. Geophys.*, 41, 1016, doi:10.1029/2002RG000123, 2003.
- Sihvola, A. and Tiuri, M.: Snow fork for field determination of the density and wetness profiles of a snow pack, *IEEE T. Geosci. Remote, GE-24*, 717–721, 1996.
- Stössel, F., Guala, M., Fierz, C., Manes, C., and Lehning, M.: Micrometeorological and morphological observations of surface hoar dynamics on a mountain snow cover, *Water Resour. Res.*, 46, W04511, doi:10.1029/2009WR008198, 2010.

- Sturm, M., Taras, B., Liston, G. E., Derksen, C., Jonas, T., and Lea, J.: Estimating snow water equivalent using snow depth data and climate classes, *J. Hydrometeor.*, 11, 1380–1394, doi:10.1175/2010JHM1202.1, 2010.
- Szymkiewicz, A. and Helmig, R.: Comparison of conductivity averaging methods for one-dimensional unsaturated flow in layered soils, *Adv. Water Resour.*, 34, 1012–1025, doi:10.1016/j.advwatres.2011.05.011, 2011.
- Techel, F. and Pielmeier, C.: Point observations of liquid water content in wet snow – investigating methodical, spatial and temporal aspects, *Cryosphere*, 5, 405–418, doi:10.5194/tc-5-405-2011, 2011.
- Techel, F., Pielmeier, C., and Schneebeli, M.: Microstructural resistance of snow following first wetting, *Cold Reg. Sci. Technol.*, 65, 382–391, doi:10.1016/j.coldregions.2010.12.006, 2011.
- van Genuchten, M. T.: A closed-form equation for predicting the hydraulic conductivity of unsaturated soils, *Soil Sci. Soc. Am. J.*, 44, 892–898, doi:10.2136/sssaj1980.03615995004400050002x, 1980.
- Vionnet, V., Brun, E., Morin, S., Boone, A., Faroux, S., Le Moigne, P., Martin, E., and Willemet, J.-M.: The detailed snowpack scheme Crocus and its implementation in SURFEX v7.2, *Geosci. Model Dev.*, 5, 773–791, doi:10.5194/gmd-5-773-2012, 2012.
- Waldner, P. A., Schneebeli, M., Schultze-Zimmermann, U., and Flüher, H.: Effect of snow structure on water flow and solute transport, *Hydrol. Proc.*, 18, 1271–1290, doi:10.1002/hyp.1401, 2004.
- Wever, N., Fierz, C., Mitterer, C., Hirashima, H., and Lehning, M.: Solving Richards Equation for snow improves snowpack meltwater runoff estimations in detailed multi-layer snowpack model, *Cryosphere*, 8, 257–274, doi:10.5194/tc-8-257-2014, 2014.
- [Wever, N.: Biweekly manual snow profiles from Weissfluhjoch, Davos, Switzerland, Dataset, WSL Institute for Snow and Avalanche Research SLF, doi:10.16904/2, 2015-09-14.](#)
- [Wever, N., Schmucki, E., and Marty, C.: Meteorological and snowpack measurements from Weissfluhjoch, Davos, Switzerland, Dataset, WSL Institute for Snow and Avalanche Research SLF, doi:10.16904/1, 2015-09-29.](#)
- Yamaguchi, S., Katsushima, T., Sato, A., and Kumakura, T.: Water retention curve of snow with different grain sizes, *Cold Reg. Sci. Technol.*, 64, 87–93, doi:10.1016/j.coldregions.2010.05.008, 2010.
- Yamaguchi, S., Watanabe, K., Katsushima, T., Sato, A., and Kumakura, T.: Dependence of the water retention curve of snow on snow characteristics, *Ann. Glaciol.*, 53, 6–12, doi:10.3189/2012AoG61A001, 2012.

Average bulk snowpack statistics for various simulation setups (bucket or Richards equation (RE) water transport scheme, snow height (HS) or precipitation (Precip) driven simulations, Y2010 (Yamaguchi et al., 2010) or Y2012 (Yamaguchi et al., 2012) water retention curves, and arithmetic or geometric mean for hydraulic conductivity) for all simulated snow seasons. Differences are calculated as modelled value minus measured value, ratios are calculated as modelled value divided by measured value. The isothermal part is only considered during the melt phase (from March to the end of the snow season). Variable Bucket RE-Y2010AM RE-Y2012AM RE-Y2012GM Bucket RE-Y2012AM RMSE HS (cm) 4.16 4.00 4.11 4.12 20.86 23.12 Difference HS (cm) 1.33 0.87 0.88 0.89 -1.23 -5.24 RMSE SWE (mm w.e.) 39.28 39.62 39.78 39.39 84.96 99.03 Difference SWE (mm w.e.) -5.67 -7.08 -9.29 -8.06 -16.14 -36.00 Ratio SWE (mm w.e.) 1.01 1.00 0.99 1.00 1.00 0.94 Ratio runoff sum (-) 1.08 1.14 1.13 1.13 0.98 0.98 NSE 24 h (-) 0.70 0.73 0.73 0.73 0.67 0.67 NSE 1 h (-) 0.12 0.57 0.58 0.58 0.05 0.42 r^2 24 h runoff sum (-) 0.83 0.85 0.85 0.85 0.84 0.83 r^2 1 h runoff sum (-) 0.47 0.75 0.75 0.75 0.47 0.69 Lag correlation for runoff (h) -1.47 -0.20 -0.17 -0.13 -1.72 -0.44 RMSE cold contents (t) 668 570 609 603 964 900 Difference cold contents (t) -103.8 34.9 -4.2 -11.1 -60.6 45.4 r^2 cold contents (-) 0.90 0.92 0.91 0.91 0.83 0.85 r^2 isothermal part (-) 0.74 0.87 0.86 0.85 0.75 0.86 r^2 avg. grain size (-) 0.75 0.74 0.74 0.74 0.63 0.61 Mass balance error (mm w.e.) 0.01 0.01 0.01 0.01 0.09 0.02 Energy balance error (t) 0.03 0.06 0.06 0.05 -0.05 0.05 CPU time (min) 0.57 1.39 1.44 1.45 0.61 1.55

Table 1. Average and standard deviation (in brackets) of bulk snowpack statistics over all snow seasons for various simulation setups (bucket or Richards equation (RE) water transport scheme, snow height (HS) or precipitation (Precip) driven simulations, Y2010 (Yamaguchi et al., 2010) or Y2012 (Yamaguchi et al., 2012) water retention curves, and arithmetic or geometric mean for hydraulic conductivity) for all simulated snow seasons. Differences are calculated as modelled value minus measured value, ratios are calculated as modelled value divided by measured value. The isothermal part is only considered during the melt phase (from March to the end of the snow season).

Variable	Bucket	HS driven (2000–2014)			Precip driven (1997–2014)	
		RE-Y2010AM	RE-Y2012AM	RE-Y2012GM	Bucket	RE-Y2012AM
RMSE HS (cm)	4.16 (1.73)	4.00 (1.56)	4.11 (1.64)	4.12 (1.71)	20.86 (12.31)	23.12 (11.38)
Difference HS (cm)	1.33 (2.24)	0.87 (2.09)	0.88 (2.17)	0.89 (2.21)	-1.23 (12.31)	-5.24 (11.38)
Difference melt out (days)	-0.67 (1.45)	-0.73 (1.44)	-0.73 (1.44)	-0.73 (1.44)	-3.94 (6.08)	-7.00 (6.83)
RMSE SWE (mm w.e.)	39.28 (15.51)	39.62 (14.71)	39.78 (15.50)	39.39 (15.45)	84.96 (36.34)	99.03 (36.23)
Difference SWE (mm w.e.)	-5.67 (27.20)	-7.08 (27.04)	-9.29 (27.05)	-8.06 (27.14)	-16.14 (67.61)	-36.00 (66.91)
Ratio SWE (mm w.e.)	1.01 (0.09)	0.99 (0.08)	0.99 (0.08)	0.99 (0.08)	0.97 (0.19)	0.91 (0.17)
Ratio runoff sum (-)	1.08 (0.28)	1.14 (0.28)	1.13 (0.28)	1.13 (0.28)	0.98 (0.31)	0.98 (0.31)
NSE 24 hours (-)	0.72 (0.32)	0.73 (0.32)	0.73 (0.32)	0.73 (0.32)	0.66 (0.32)	0.67 (0.31)
NSE 1 hour (-)	0.13 (0.37)	0.57 (0.35)	0.59 (0.34)	0.58 (0.34)	0.02 (0.39)	0.39 (0.34)
r^2 24 hrs runoff sum (-)	0.85 (0.11)	0.87 (0.10)	0.87 (0.10)	0.87 (0.10)	0.84 (0.12)	0.85 (0.13)
r^2 1 hour runoff sum (-)	0.52 (0.06)	0.78 (0.08)	0.78 (0.08)	0.78 (0.08)	0.48 (0.07)	0.68 (0.11)
Lag correlation for runoff (h)	-1.47 (0.79)	-0.20 (0.37)	-0.17 (0.31)	-0.13 (0.30)	-1.72 (0.79)	-0.44 (0.48)
RMSE cold contents (kJ m ⁻²)	627 (274)	529 (244)	554 (285)	551 (277)	786 (556)	742 (509)
Difference cold contents (kJ m ⁻²)	-129.0 (312.9)	11.1 (326.2)	-30.5 (336.2)	-36.7 (322.9)	-46.0 (604.0)	62.4 (565.0)
r^2 cold contents (-)	0.76 (0.36)	0.78 (0.36)	0.79 (0.36)	0.78 (0.36)	0.77 (0.36)	0.78 (0.36)
r^2 isothermal part (-)	0.64 (0.33)	0.74 (0.36)	0.74 (0.36)	0.73 (0.35)	0.65 (0.32)	0.74 (0.36)
r^2 avg. grain size (-)	0.47 (0.31)	0.45 (0.30)	0.45 (0.30)	0.45 (0.30)	0.39 (0.29)	0.37 (0.28)
Mass balance error (mm w.e.)	0.01 (0.00)	0.01 (0.00)	0.01 (0.00)	0.01 (0.00)	0.09 (0.25)	0.02 (0.03)
Energy balance error (W m ⁻²)	0.03 (0.08)	0.06 (0.08)	0.06 (0.08)	0.05 (0.08)	-0.05 (0.07)	0.05 (0.08)
CPU time (min)	0.57 (0.07)	1.39 (0.26)	1.44 (0.36)	1.45 (0.37)	0.61 (0.11)	1.55 (0.45)

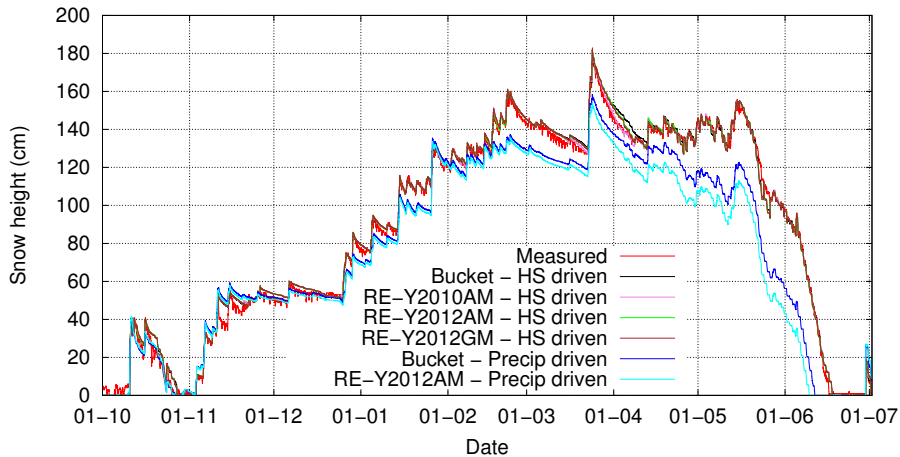


Figure 1. Measured and modelled snow height for different model setups (bucket or Richards equation (RE) water transport scheme, snow height (HS) or [precipitation](#) ([precipitation](#)) (Precip) driven simulations, Y2010 (Yamaguchi et al., 2010) or Y2012 (Yamaguchi et al., 2012) water retention curves, and arithmetic (AM) or geometric mean (GM) for hydraulic conductivity) for the example snow season 2014, from October 2013 to July 2014. [Note that apart from forcing with either snow height or precipitation measurements, differences between simulation setups cause only small differences in snow height simulations, resulting in overlapping lines in the figure.](#)

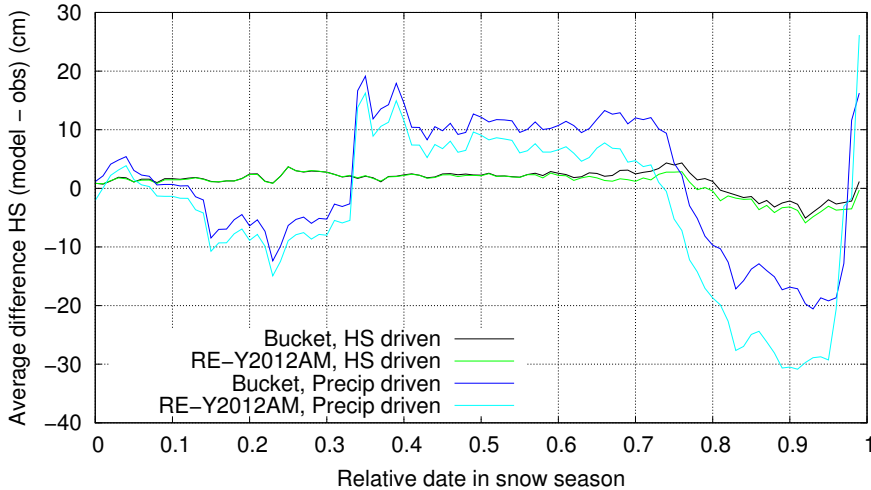


Figure 2. Difference in modelled and measured snow height relative to the snow season for both snow height (HS) and precipitation (Precip)-driven simulations, determined over 15 and 18 years, respectively, using the bucket scheme or Richards equation with Yamaguchi et al. (2012) water retention curve and arithmetic mean for hydraulic conductivity (RE-Y2012AM). For every snow season, the first day with a snow cover is set at 0, the last day at 1.

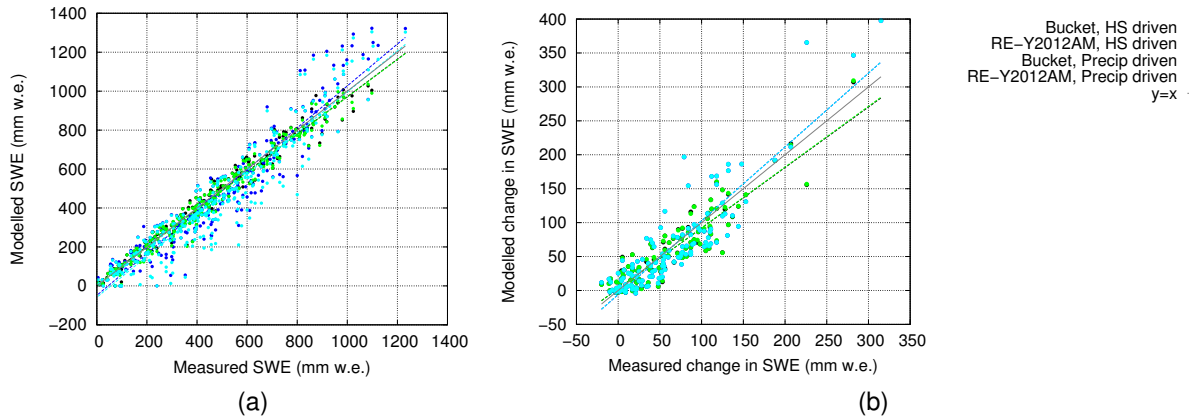


Figure 3. Comparison of measured and modelled SWE (mm w.e.) **(a)** and increase in SWE in the biweekly profiles and the simulations during the accumulation phase **(b)** for both snow height (HS) and precipitation (Precip)-driven simulations, using the bucket scheme or Richards equation with Yamaguchi et al. (2012) water retention curve and arithmetic mean for hydraulic conductivity (RE-Y2012AM). Coloured lines denote the linear fits to the corresponding data, the black line indicates the line $y = x$. The blue and cyan dots in **(b)** perfectly overlap.

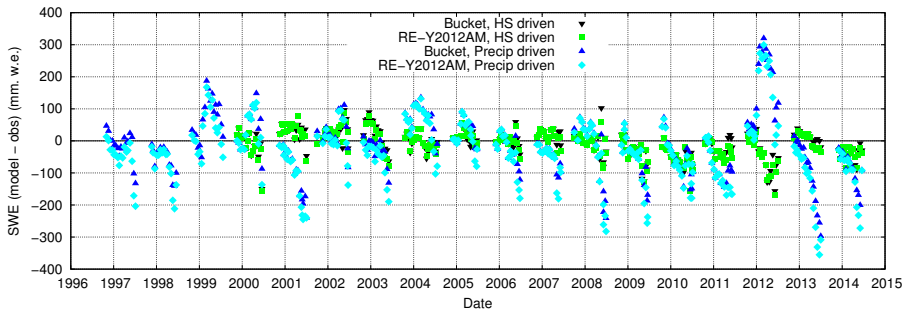
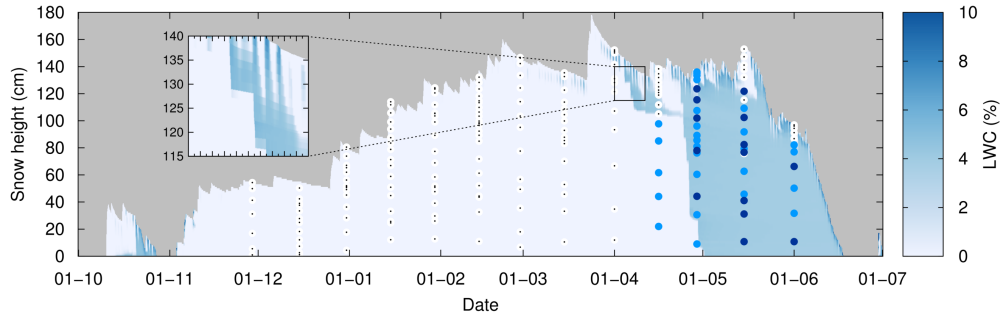
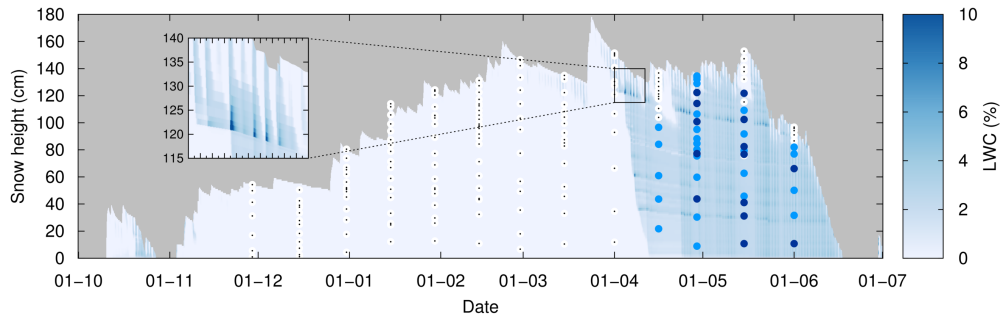


Figure 4. Difference in modelled and observed SWE in the biweekly profiles for both snow height (HS) and precipitation (Precip)-driven simulations, using the bucket scheme or Richards equation with Yamaguchi et al. (2012) water retention curve and arithmetic mean for hydraulic conductivity (RE-Y2012AM).



(a)



(b)

Figure 5. Snow LWC (%) for the snow height-driven simulation with the bucket scheme **(a)** and with Richards equation using the Yamaguchi et al. (2012) water retention curve and arithmetic mean for hydraulic conductivity (RE-Y2012AM, **(b)**), for the example snow season 2014. Dots denote layers that have been reported as dry (0% LWC, white with black center dot), moist (0-3% LWC, light blue) or wet, very wet or soaked ($\geq 3\%$ LWC, dark blue) from the biweekly snow profiles. When layers are reported as "1-2" (dry-moist), it is considered moist. In the zoom insert, major and minor x-axis ticks denote midnight and noon, respectively.

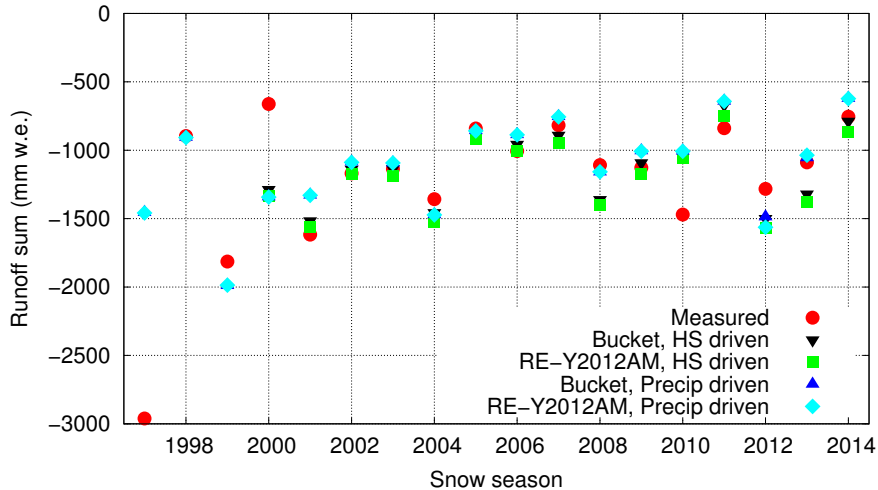
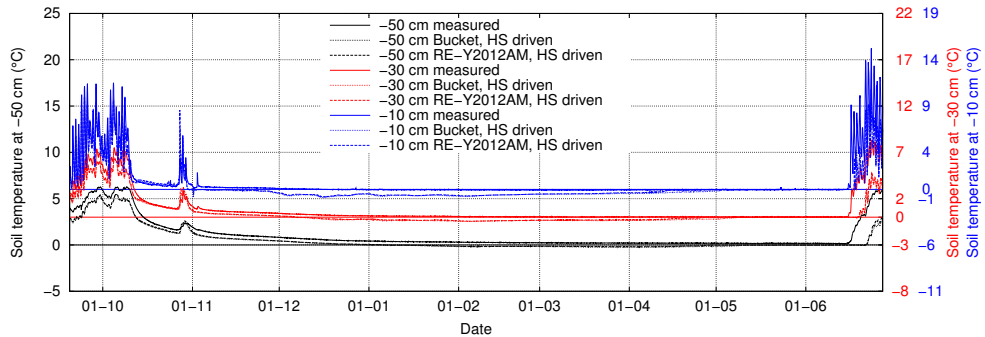
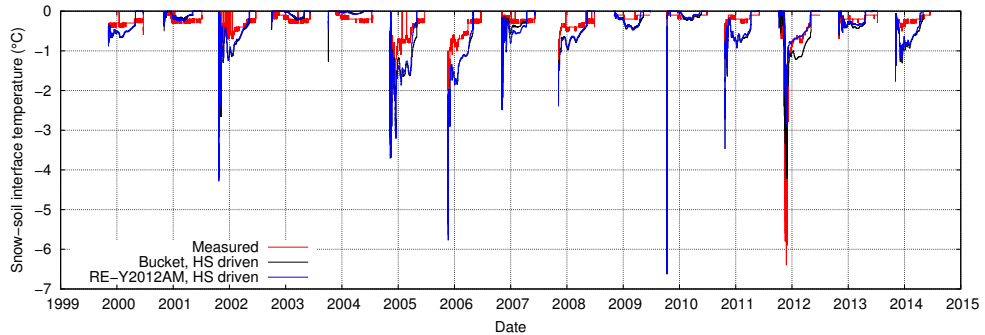


Figure 6. Snow LWG Seasonal runoff sums (mm) for the snow height-driven simulation with from the bucket scheme (a) and with Richards equation using perspective of the Yamaguchi et al. (2012) water retention curve and arithmetic mean for hydraulic conductivity snowpack mass balance (RE-Y2012AM, (b), for the example snow season 2014. negative values denote snowpack outflow).



(a)



(b)

Figure 7. Measured and modelled soil temperatures at 10, 30 and 50 cm below the surface for the example snow season 2014 (a) and measured and modelled snow–soil interface temperature for snow seasons 2000–2014 (b). Only the snow height-driven (HS driven) simulations with the bucket scheme and Richards equation using the Yamaguchi et al. (2012) water retention curve and arithmetic mean for hydraulic conductivity (RE-Y2012AM) are shown. Note that the x-axes for 30 and 50 cm depth are staggered by 3 °C to prevent overlap.

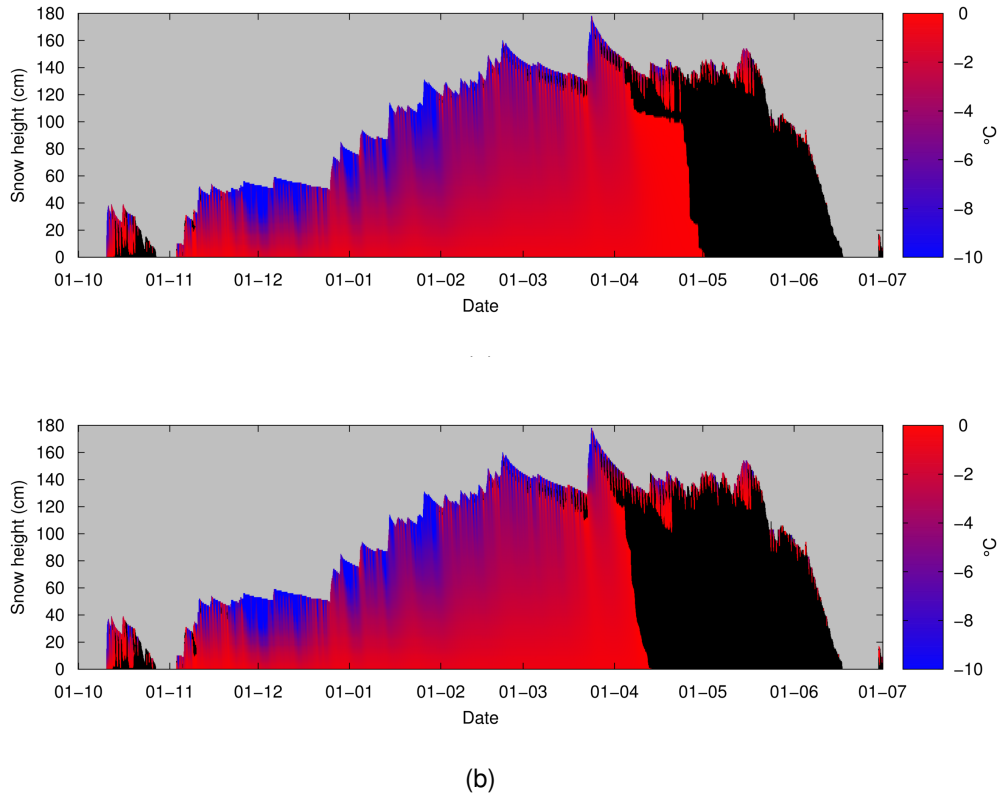


Figure 8. Snow temperature ($^{\circ}\text{C}$) for the snow height-driven simulation with the bucket scheme **(a)** and with Richards equation using the Yamaguchi et al. (2012) water retention curve and arithmetic mean for hydraulic conductivity (RE-Y2012AM, **(b)**), for example snow season 2014. Snow at exactly 0°C is coloured black to mark areas of the snowpack that are melting or freezing.

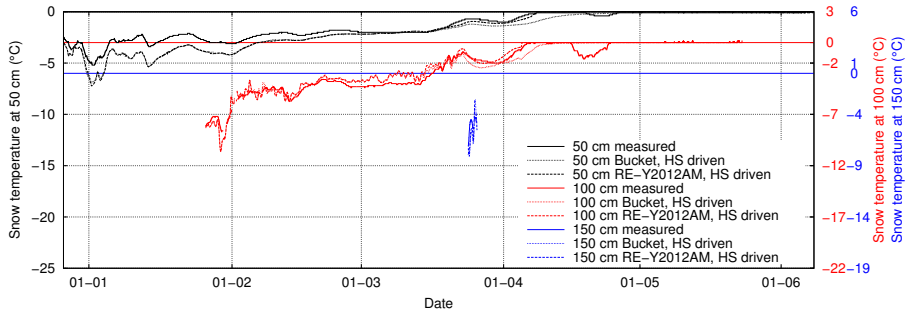


Figure 9. Measured and modelled snow temperatures at 50, 100 and 150 cm above the ground for snow height-driven (HS driven) simulations using the bucket scheme or Richards equation using the Yamaguchi et al. (2012) water retention curve and arithmetic mean for hydraulic conductivity (RE-Y2012AM) for the example snow season 2014. Values are only plotted when the snow height was at least 20 cm more than the height of the temperature sensor. Note that the x-axes for 100 and 150 cm depth are staggered by 3 °C to prevent overlap.

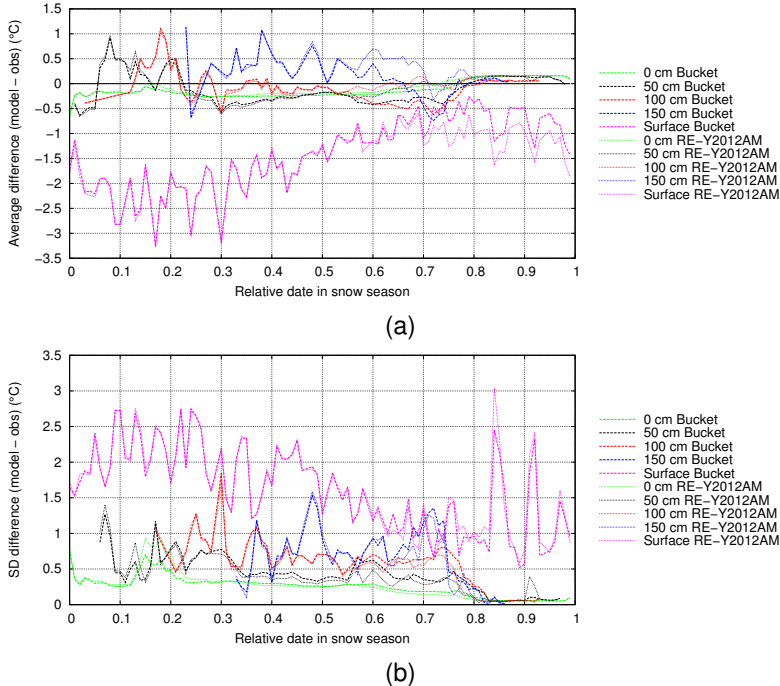
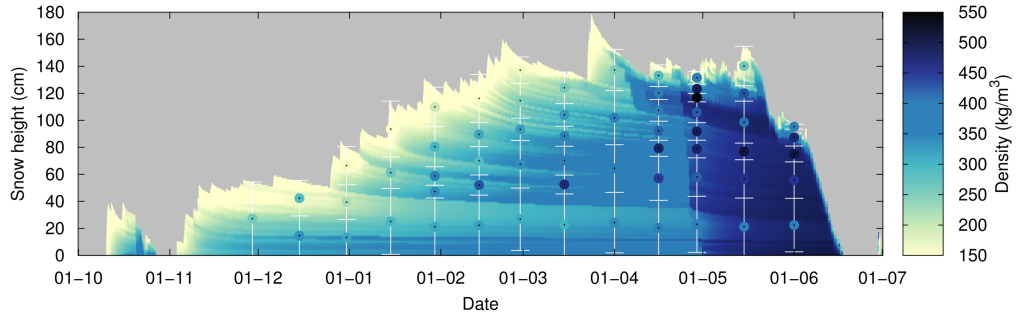
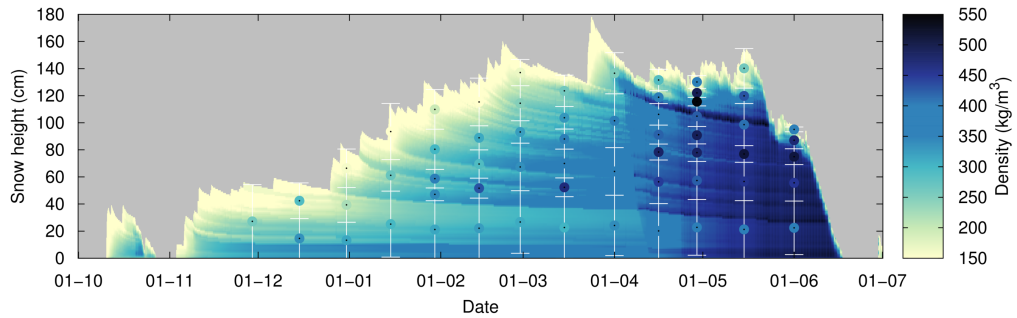


Figure 10. Average (a) and SD (b) of the difference between modelled and measured snow temperatures, surface temperature and ground temperature (°C) relative to the snow season. For every snow season, the first day with a snow cover is set at 0, the last day at 1. The statistics are determined over the 15 snow seasons of the snow height-driven simulations using the bucket scheme or Richards equation using the Yamaguchi et al. (2012) water retention curve and arithmetic mean for hydraulic conductivity (RE-Y2012AM).



(a)



(b)

Figure 11. Snow density (kg m^{-3}) for the snow height-driven simulation with the bucket scheme **(a)** and with Richards equation using the Yamaguchi et al. (2012) water retention curve and arithmetic mean for hydraulic conductivity (RE-Y2012AM, **(b)**), for example snow season 2014. Dots with a black center point indicate measured snow density reported from the biweekly snow profiles, where the black center point is located in the middle of the observed layer and the white bars denote the extent of the layer of the respective density measurement.

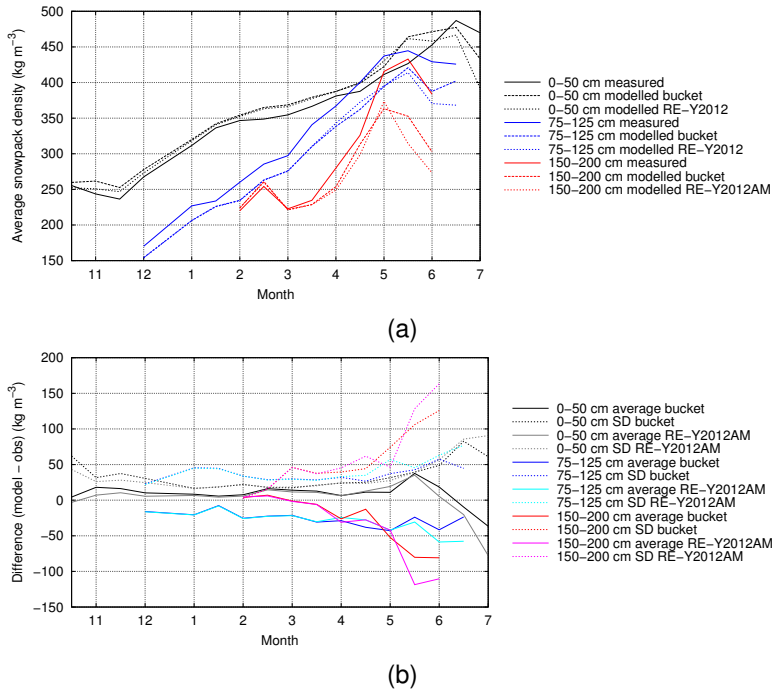
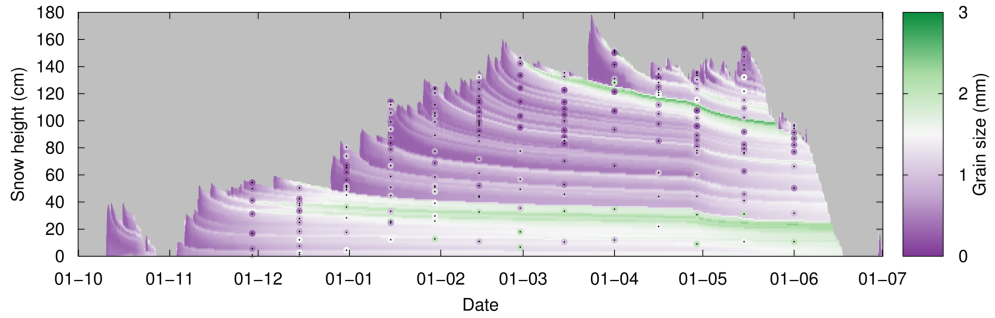
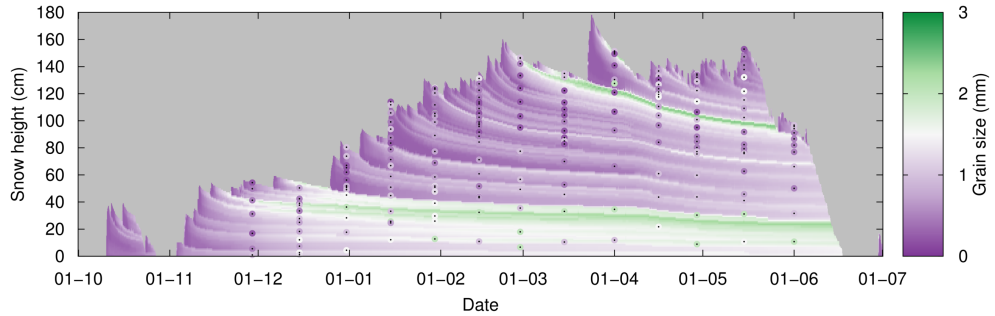


Figure 12. Average simulated and measured snow density (kg m^{-3}) **(a)** and average and SD of the difference between simulated and measured snow density (kg m^{-3}) **(b)**, **relative to the snow season** for the lower, middle and upper part of the snowpack. **For every snow season, the first day with a snow cover is set at 0, the last day at 1.** The statistics are determined over the 15 snow seasons of the snow height-driven simulations using the bucket scheme or Richards equation using the Yamaguchi et al. (2012) water retention curve and arithmetic mean for hydraulic conductivity (RE-Y2012AM).



(a)



(b)

Figure 13. Grain size (mm) for the snow height-driven simulation with the bucket scheme **(a)** and with Richards equation using the Yamaguchi et al. (2012) water retention curve and arithmetic mean for hydraulic conductivity (RE-Y2012AM, **(b)**), for the example snow season 2014. Dots with a black center point indicate observed grain sizes reported from the biweekly snow profiles, where the black center point is located in the middle of the observed layer.

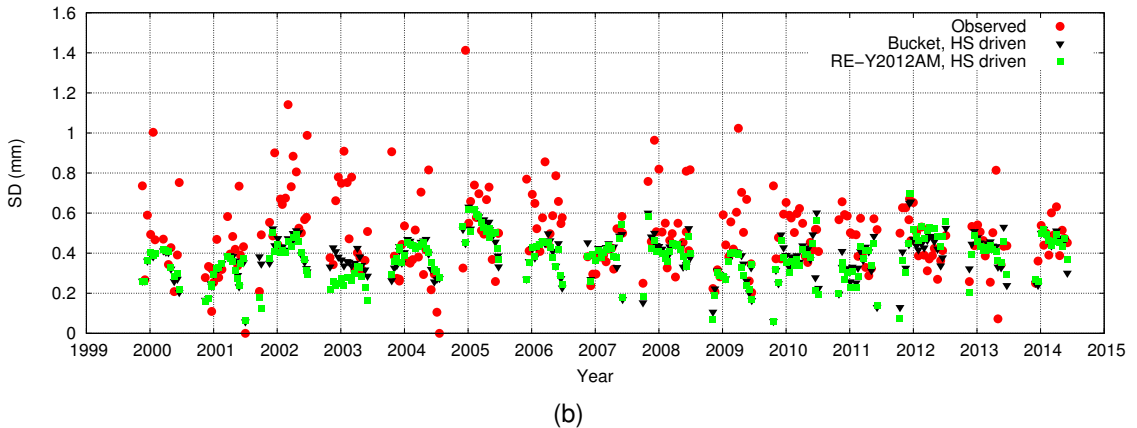
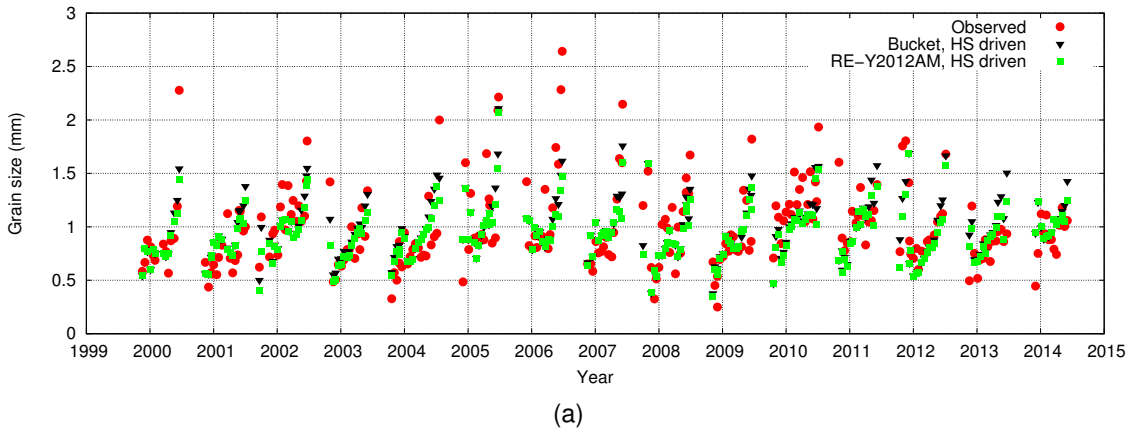
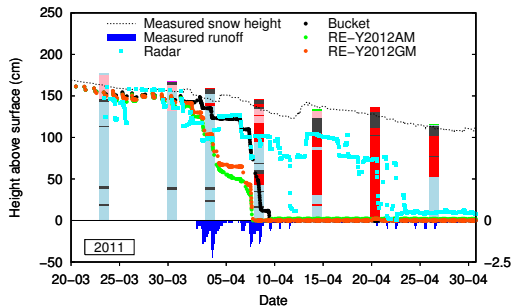
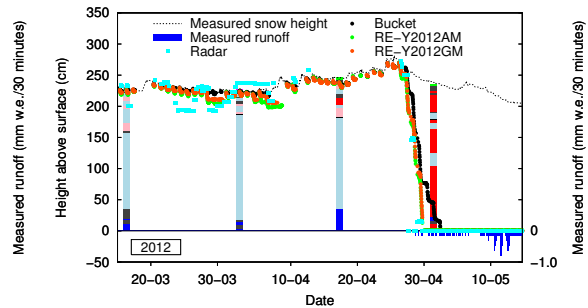


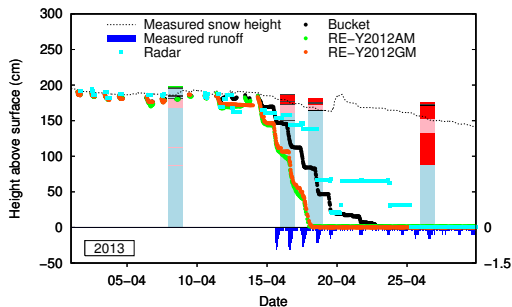
Figure 14. Average (a) and SD (b) of observed and modelled grain size (mm) from snow height driven (HS) simulations using both the Bucket scheme and Richards equation using the Yamaguchi et al. (2012) water retention curve and arithmetic mean for hydraulic conductivity (RE-Y2012AM).



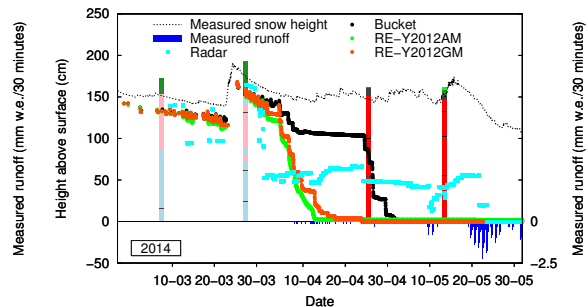
(a)



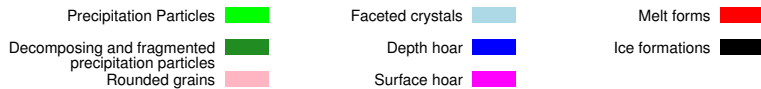
(b)



(c)



(d)



(e)

Figure 15. Snow height (dashed line), manual snow profiles (coloured bars, legend provided in **e**) and the position of the meltwater front as detected from the upGPR data (cyan dots), modelled with the bucket scheme (black dots), Richards equation with Yamaguchi et al. (2012) water retention curve and arithmetic mean for hydraulic conductivity (RE-Y2012AM, green dots) and similar but with geometric mean (RE-Y2012GM, brown dots) for snow season 2011 (**a**), 2012 (**b**), 2013 (**c**) and 2014 (**d**). Measured snowpack runoff is denoted by blue bars. The simulations were snow height-driven.